Geoderma 380 (2020) 114637

Contents lists available at ScienceDirect

Geoderma

journal homepage: www.elsevier.com/locate/geoderma

# Effects of commonly used nitrification inhibitors—dicyandiamide (DCD), 3, 4-dimethylpyrazole phosphate (DMPP), and nitrapyrin—on soil nitrogen dynamics and nitrifiers in three typical paddy soils

Xue Zhou[a,b,c], Shuwei Wang[d,e,f], Shutan Ma[g], Xinkun Zheng[c], Zhiyuan Wang[h], Chunhui Lu[b,c,*]

[a] College of Agricultural Engineering, Hohai University, Nanjing 210098, Jiangsu Province, China
[b] Yangtze Institute for Conservation and Development, Hohai University, Nanjing 210098, Jiangsu Province, China
[c] State Key Laboratory of Hydrology-Water Resources and Hydraulic Engineering, Hohai University, Nanjing 210098, Jiangsu Province, China
[d] State Key Laboratory of Soil and Sustainable Agriculture, Institute of Soil Science, Chinese Academy of Sciences, Nanjing 210008, China
[e] University of Chinese Academy of Sciences, Beijing 100049, China
[f] Changshu Agro-ecological Experimental Station, Chinese Academy of Sciences, Changshu 215555, China
[g] School of Environmental Science and Engineering, Anhui Normal University, Wuhu 241000, Anhui Province, China
[h] Center for Eco-Environmental Research, Nanjing Hydraulic Research Institute, Nanjing 210029, China

ARTICLE INFO

Handling Editor: Dr. Jan Willem Van Groenigen

ABSTRACT

The use of nitrification inhibitors (NIs) with ammonium ($NH_4^+$) -based fertilizers is an efficient strategy for reducing nitrogen (N) loss by affecting ammonia-oxidizing archaea (AOA) and ammonia-oxidizing bacteria (AOB) in agricultural soils. The inhibition mechanisms of NIs on AOA and AOB are still debated, as some studies have demonstrated that NIs inhibited functionally dominant groups, while others have reported selective inhibition of AOB rather than AOA. Here, we identified the impacts of the most commonly used NIs (dicyandiamide (DCD), 3,4-dimethylpyrazole phosphate (DMPP) and nitrapyrin) on the nitrification activity, $N_2O$ emission, and abundance and metabolic activity of ammonia oxidizers (AOA, AOB, and comammox (detected only in HL)) in three paddy soils (HL, JX, and SC) with distinct properties using microcosm incubation combined with the $^{13}CO_2$-DNA-stable isotope probing (SIP) technique. Most of the NIs treatments effectively inhibited the $N_2O$ emission with efficacy suppressed the metabolic activity of AOB, regardless of soil type and NI type, whereas the nitrification process and AOA activity could not be inhibited. The efficacy of NIs was also dependent on soil chemical properties, as nitrapyrin did not inhibit AOB growth at the beginning of microcosm incubation in HL, and DCD successfully inhibited the activity of both AOA and AOB in JX. In HL, DCD and DMPP effectively inhibited the activity of comammox, while nitrapyrin could not inhibit its activity. This study is the first to identify the response pattern of comammox to DCD, DMPP, and nitrapyrin in paddy soil by DNA-SIP microcosm incubation. This study also suggested that NIs might selectively inhibit AOB rather than AOA.

## 1. Introduction

Nitrogen (N) is an essential element for plant growth, and N-based fertilizers are used extensively in agriculture to promote plant growth. The soil nitrification process, involving the transformation of ammonia ($NH_3$) to nitrate ($NO_3^-$) via nitrite ($NO_2^-$) by microorganisms, limits the effectiveness of much of the applied N fertilizer, either directly or indirectly leads to $NO_3^-$ leaching (Schlesinger, 2009) and nitrous oxide ($N_2O$) emission (Hu et al., 2015a), and affects the emission of other reactive N pollutants such as nitric oxide (NO) or ammonia ($NH_3$) (Li et al., 2020; Medinets et al., 2015; Ussiri and Lal, 2012; Xu et al., 2012). The $NO_3^-$ leaching causes groundwater pollution and eutrophication. The $N_2O$ has a global warming potential 298 times that of $CO_2$ (Ravishankara et al., 2009). Thus, reducing nitrification is a pressing need for sustainable agricultural management practices. The application of nitrification inhibitors (NIs) with N fertilizers is currently being explored as an effective strategy for slowing the microbial conversion of $NH_3$ to $NO_3^-$, reducing N loss and $N_2O$ emission from agricultural systems and thereby promoting N use efficiency (Dinnes et al., 2002).

The $NH_3$ oxidation, catalyzed by ammonia monooxygenase (AMO), is the first and rate-limiting step of nitrification. Ammonia monooxygenase (AMO) is encoded by the *amoA* gene and is present in ammonia-oxidizing archaea (AOA), ammonia-oxidizing bacteria (AOB) and comammox bacteria (a newly discovered completely nitrifying

* Corresponding author at: Yangtze Institute for Conservation and Development, Hohai University, Nanjing 210098, Jiangsu Province, China.
*E-mail address:* clu@hhu.edu.cn (C. Lu).

https://doi.org/10.1016/j.geoderma.2020.114637
Received 12 July 2019; Received in revised form 13 July 2020; Accepted 28 July 2020

bacteria) (Daims et al., 2015; Daims et al., 2016; van Kessel et al., 2015). In agriculture, dicyandiamide (DCD), 3,4-dimethylpyrazole phosphate (DMPP) and 2-chloro-6-(trichloromethyl) pyridine (nitrapyrin) are commercially-used nitrification inhibitors (NIs) (Di and Cameron, 2018). The mode of action for NIs have been assumed: DCD and DMPP are thought to be Cu-chelating agents acting on AMO (Morales et al., 2015); nitrapyrin suppresses the activity of ammonia oxidizers by blocking the AMO enzymatic pathway (Subbarao et al., 2009; Subbarao et al., 2008). Understanding the inhibitory mechanism of these NIs may help to optimize the application and thus increase the efficiency of these NIs during agricultural management.

To reveal the effect of NIs on microbes, field- and laboratory-based studies have explored the influence of NIs on the abundance, diversity and community structure of ammonia oxidizers. Due to the variable responses of AOA and AOB communities to NIs application, the inhibitory mechanism is still debated. According to the published results regarding the impacts of NIs on the ammonia oxidizers, we assumed two possible inhibitory mechanisms of NIs.

Hypothesis 1: The NIs only inhibited the functionally dominant groups. The Differences in cellular biochemistry and metabolism have been demonstrated between AOA and AOB (Kozlowski et al., 2016; Prosser and Nicol, 2012), leading to the niche and activity differentiation of AOA and AOB in the environments with different chemical properties. For example, soil pH and substrate concentration are critical factors driving the niche partitioning of AOB and AOA (Hu et al., 2015b; Prosser and Nicol, 2012); AOA grew preferentially in acidic soils with lower nutrient availability, while AOB grew preferentially in soils with high $NH_3$ concentration and relatively high pH. As a consequence, NIs selectively inhibited the active ammonia oxidizers in the soils with different physio-chemical properties. For example, NIs decreased both AOB and AOA *amoA* gene abundance and inhibited their activity in the soils where AOA and AOB were active (Di and Cameron, 2011; Dong et al., 2013b; Florio et al., 2014; Gong et al., 2013). However, in acidic soils where AOA were active rather than AOB, the inhibitory effect of NIs were only observed on AOA (Gu et al., 2019; Zhang et al., 2012).

Hypothesis 2: The NIs selectively inhibited AOB in soils where AOA remained active. DCD, DMPP and nitrapyrin are suggested to act as metal chelators by binding copper in the active site of the amoB subunit of ammonia oxidizers (McCarty, 1999; Ruser and Schulz, 2015). However, differences in the cellular structure and the $NH_3$ oxidation pathways of AOA and AOB indicated that periplasmic amoB presumably contained an active site that catalyzes reactions using copper for AOB (Balasubramanian et al., 2010), whereas activity assays of isolated archaeal amoB indicated an inactive enzyme (Lawton et al., 2014), and the amoC or the amoX subunit might serve as the active site for AOA (Tolar et al., 2017). Thus, NIs might be effective on inhibiting AOB rather than AOA. A large number of studies showed that NIs effectively decreased the abundance of AOB and suppressed its metabolic activity, while AOA was shown to still be active (Chen et al., 2019; Fan et al., 2019; Fu et al., 2018; Kleineidam et al., 2011; Lan et al., 2018; Shi et al., 2016a; Shi et al., 2016b).

It is notable that we could not conclude Hypothesis 2 from some results where AOB contributed to the nitrification processes but AOA was not active. Although NIs inhibited only AOB growth, it is not clear whether the inhibition effect is the result of the selective inhibition of AOB or inhibition of the active ammonia oxidizers. For example, both DMPP and DCD were highly effective in inhibiting the growth of AOB, thus significantly slowing down $NH_4^+$ oxidation in six new Zealand grazed grassland soils, where AOA were not active (Di and Cameron, 2011). Similarly, DMPP significantly reduced AOB *amoA* gene copy number (Dong et al., 2013a; Duan et al., 2017; Li et al., 2019b; Zhang et al., 2018), while AOA also did not respond to the application of urea. The increased suppression of the AOB population size by DCD was observed (Wang et al., 2016a) (Dai et al., 2013; Di et al., 2009; Gong et al., 2013; Wang et al., 2017a), where AOA did not show any contribution to nitrification. Due to the unclear inhibition mechanisms described above, there is an urgent need for more investigations of the effect of NIs on the ammonia oxidizers in soils with different properties.

Furthermore, the existence of the comammox Nitrospira, which performs complete $NH_3$ oxidation all the way to $NO_3^-$, was confirmed in late 2015 (Daims et al., 2015; van Kessel et al., 2015). This discovery overturned a > 100-year paradigm in which nitrification is a two-step process conducted by ammonia-oxidizing microbes (AOB and AOA) and nitrite-oxidizing bacteria (NOB). Recent studies have established the activity of comammox in soils by the DNA-SIP technique (Li et al., 2019a; Wang et al., 2019). To the best of our knowledge, no information is currently available regarding the response patterns of active comammox to DCD, DMPP and nitrapyrin application. Thus, an examination of the effects of these NIs on ammonia oxidizers is needed. The comammox Nitrospira has been observed in HL soil (alkaline, relatively high organic content) in our pre-experiment.

In addition to the differentiation in active microbes might influence the performance of NIs, the efficacy of NIs was also highly influenced by soil type (physio-chemical properties) through soil physical processes (Guardia et al., 2018). For example, the sorption of NIs to the soil matrix (i.e., clays and organic matter) may decrease the NI efficacy, which was higher for DCD than DMPP (Marsden et al., 2016). Soil pH also influenced the NI efficacy; for example, higher sorption of DCD has been found in a more alkaline soil (Zhang et al., 2004), and significant higher efficacy of NIs was demonstrated in an acidic grassland soil with low CEC (cation exchange capacity) and clay content (Guardia et al., 2018).

This study was designed to determine the impact of three NIs (DCD, DMPP, and nitrapyrin) on nitrification rate, $N_2O$ emission, and the abundance of AOA, AOB and comammox (comammox was detected only in HL) in three paddy soils with distinct properties. Then, DNA-stable isotope probing (SIP) technology was employed to identify active microbes and to obtain detailed insights into the metabolic response of ammonia oxidizers to NIs in HL and JX. DNA-SIP is a culture-independent technique that is capable of linking microbial function with taxonomic identity and facilitating deep insight into the metabolic response of ammonia oxidizers to NI application. We hypothesized that (i) different NIs would have different effects on the N dynamics and microbial communities of ammonia oxidizers and that (ii) ammonia oxidizers would present contrasting response patterns in soils with different properties owing to the potential activity differentiation of ammonia oxidizers.

## 2. Materials and methods

### 2.1. Sample collection

Soil samples (0–20 cm depth) were collected from paddy fields in Heilongjiang, Jiangxi, and Sichuan Province, China, in September 2016. The sampling sites were planted with rice for over 20 years and regularly fertilized. The soils were classified as black soil (HL), red soil (JX) and purple soil (SC). For each soil, six cores were collected, mixed and homogenized. The soil samples were transported on ice to the laboratory and passed through a 2-mm sieve. Then, the samples were stored at 4 °C for soil property analysis and microcosm incubation.

The soil water content was measured at 105 °C for 24 h. The soil pH was determined in 2.5:1 (w:v) ratios of soil to distilled water using a DMP-2 mV pH detector (Quark Ltd., Nanjing, China). The soil organic carbon (SOC) content was analyzed by wet digestion with $H_2SO_4$-$K_2Cr_2O_7$. Soil was homogenized with 2 M KCl (soil/KCl, 1:5) by shaking at 200 rpm for 30 min and then passed through filter paper for determination of $NH_4^+$-N, $NO_2^-$-N and $NO_3^-$-N levels using a Skalar SAN Plus segmented flow analyzer (Skalar Inc., Breda, The Netherlands). The chemical properties of the soils in this study were established and are listed in Table 1. The pH in HL and SC soil were 7.5 and 6.9, and the pH in JX soil was 5.3. The HL soil had a relatively high organic content, whereas the JX and SC soils had a relatively low organic content.

**Table 1**
Basic properties and nitrifiers (AOA, AOB and comammox) abundance of the soils in this study.

| Property | HL | JX | SC |
|---|---|---|---|
| pH | 7.5 ± 0.2a | 5.3 ± 0.2c | 6.9 ± 0.2b |
| $NH_4^+$-N (mg $kg^{-1}$) | 159.2 ± 4.6a | 161.6 ± 5.0a | 31.1 ± 4.8b |
| $NO_3^-$-N (mg $kg^{-1}$) | 29.9 ± 7.2b | 14.1 ± 0.8c | 72.9 ± 7.4a |
| Total C (%) | 8.2 ± 0.2a | 1.4 ± 0.1b | 1.4 ± 0.1b |
| soil texture | Loam clay | Loam clay | Loam clay |
| bulk density (g $cm^{-3}$) | 1.37 | 1.26 | 1.42 |
| CEC (cmol $kg^{-1}$) | 33.0 | 8.3 | 26.2 |
| AOA (copies $g^{-1}$ $soil_{dw}$) | $1.85 \times 10^5 \pm 7.30 \times 10^2$a | $4.69 \times 10^4 \pm 8.64 \times 10^2$b | $2.36 \times 10^5 \pm 1.15 \times 10^4$a |
| AOB (copies $g^{-1}$ $soil_{dw}$) | $1.85 \times 10^5 \pm 5.62 \times 10^3$a | $3.86 \times 10^3 \pm 1.48 \times 10^2$c | $3.97 \times 10^4 \pm 3.61 \times 10^3$b |
| comammox (copies $g^{-1}$ $soil_{dw}$) | $3.11 \times 10^5 \pm 1.75 \times 10^4$ | – | – |

### 2.2. Microcosm incubation

For each soil, five treatments, namely, the water (control), 200 mg $kg^{-1}$ urea-N (urea), 200 mg $kg^{-1}$ urea-N + DCD (10% urea-N) (DCD), 200 mg $kg^{-1}$ urea-N + DMPP (1% urea-N) (DMPP), and 200 mg $kg^{-1}$ urea-N + nitrapyrin (0.1% urea-N) (nitrapyrin), were applied to each soil in triplicate. Fresh soil (equivalent to 10.0 g of dry weight per gram of soil) was incubated and solutions were added that the final soil moisture was 40% of maximum water-holding capacity (about 50% WFPS) in 100-mL serum bottles (Xia et al., 2011). Soil samples were thoroughly mixed with a composite of urea, DCD, DMPP and nitrapyrin, respectively, and the bottles were tightly capped with black butyl stoppers and incubated at 28 °C.

Water loss was replaced by adding sterilized water. Destructive sampling of each soil sample was conducted in triplicate on days 0, 7, 14, and 28. At each time point, before removing the butyl stoppers, gas was extracted using a gas-tight syringe and injected into 10-mLp vacuum exetainers. The $N_2O$ analysis was performed on a gas chromatograph (Agilent 7890A, Agilent Technologies, Inc., USA) with ECD detector. The $N_2O$ fluxes were calculated based on the Eq. (1) described below:

$$F = (\rho \times \Delta C \times V \times 273)/[W \times \Delta t \times (273 + T)] \quad (1)$$

where F: gas emission rate, ng kg $h^{-1}$ ($N_2O$-N); ρ: gas density, 1.25 kg $m^{-3}$ ($N_2O$-N); V: headspace of the bottle, $m^3$; W: soil dry weight, kg; ΔC: gas concentration; Δt: sampling interval; and T: incubation temperature, °C.

Then, the headspace of the bottle was flushed weekly with pressurized synthetic air (20% $O_2$, 80% $N_2$) for 1 min to maintain oxic conditions. Approximately 5.0 g of fresh soil was removed from each replicate and immediately frozen at −20 °C for molecular analysis. The remainder of each replicate soil sample was used for analysis of inorganic N content.

### 2.3. Nucleic acid extraction and quantitative PCR

Soil nucleic acid was extracted from 0.5 g of soil using a FastDNA SPIN Kit for Soil (MPbio, USA) according to the manufacturer's instruction. DNA was stored at −20 °C. The population sizes of AOA and AOB were assessed by quantification of *amoA* gene copies in soil samples using the primer pairs Arch-amoAF/Arch-amoAR (Francis et al., 2005) and amoA-1F/amoA-2R (Rotthauwe et al., 1997), respectively (Table S1). The population sizes of comammox bacterial clade A *amoA* and comammox bacterial clade B *amoA* were measured using mixtures of the primer pairs comA-244f_(a-f)/comA-659r_(a-f) and comB-244f_(a-f)/comB-659r_(a-f), respectively (Pjevac et al., 2017). However, in our previous research (unpublished), PCR amplification using the primers comA and comB yielded some amplification products, as determined by agarose gel electrophoresis, did not belong to the comammox Nitrospira by clone sequencing and phylogenetic analysis. Thus, to ensure the accuracy of the qPCR results, we chose only the samples that yielded the comammox Nitrospira *amoA* gene amplicons (Fig. S1) for the subsequent qPCR analysis of comammox. Real-time quantitative PCR was carried out on a CFX96 optical real-time detection system (Bio-Rad Laboratories, Inc., Hercules, CA). The DNA templates were diluted 10-fold to 1–10 ng in each reaction mixture to avoid possible inhibition by coextracted humic substances. Quantitative PCR was performed in 20-μL reaction mixtures containing 10 μL of 2x SYBR Premix Ex Taq (Takara Biotech, Dalian, China), 200 nM each primer, and 20 ng of DNA template. The thermal program for the real-time PCR assay is provided in Table S1. Blanks were run as negative controls with water as the template instead of soil DNA extract. Standard curves were constructed by using a dilution series ($10^7$-$10^1$) of plasmids harboring the *amoA* gene. Plasmids were extracted by a Plasmid Purification Kit (Takara), and the concentrations were measured by using a Nanodrop ND-1000 UV–vis spectrophotometer and used to calculate standard copy numbers. The amplification efficiency ranged from 83.5% to 95.0%, with $R^2$ values of approximately 0.99 in each reaction.

### 2.4. DNA-SIP microcosm incubation and analysis

Based on the distinct $N_2O$ emission patterns and nitrification activities in alkaline and neutral soils (HL and SC) and acidic soil (JX) as described in Result Section, HL and JX soils were chosen for DNA-SIP microcosm incubation. For each soil, four treatments, namely, a $^{13}CO_2$-labeled treatment ($^{13}CO_2$ + 200 mg $kg^{-1}$ urea-N (urea)) and control treatments ($^{13}CO_2$ + 200 mg $kg^{-1}$ urea-N + DCD (10% urea-N) (DCD), $^{13}CO_2$ + 200 mg $kg^{-1}$ urea-N + DMPP (1% urea-N) (DMPP), and $^{13}CO_2$ + 200 mg $kg^{-1}$ urea-N + nitrapyrin (0.1% urea-N) (nitrapyrin)) were applied.

Briefly, the soils (equivalent to 10.0 g of dry weight per gram of soil, i.e., d.w.s.) were incubated for 4 weeks at 28 °C in 120-mL serum bottles capped with black butyl stoppers, as described in M&M Section 2.2. The headspace of the bottle was renewed weekly with pressurized synthetic air (20% $O_2$, 80% $N_2$) and 200 μg of urea-N/g of d.w.s. Urea was added at the beginning of the incubation period. Additionally, 5% $^{13}CO_2$ was injected into the bottles and renewed once a week. The labeled $^{13}CO_2$ (99 atom% carbon) was purchased from the Shanghai Engineering Research Center for Stable Isotopes. $N_2O$ was measured once per week (day 7, 14, 21 and 28) as described in Section 2.2. Destructive sampling of 5.0 g of fresh soil from each microcosm was performed on days 0, 7, 14 and 28, and the samples were frozen immediately at −20 °C. The remaining soil was mixed with 15 mL of 2 M KCl and passed through filter paper after shaking at 200 rpm for 30 min. The concentrations of $NH_4^+$-N, $NO_2^-$-N, and $NO_3^-$-N were measured as described above.

Genomic DNA was extracted from the SIP microcosms as described above. Then, the total DNA was fractionated in triplicate as described previously (Xia et al., 2011) to resolve $^{13}$C-DNA from $^{12}$C-DNA in soils from the four treatments. Approximately 2.0 μg of DNA from each soil microcosm was mixed with a CsCl stock solution to form a CsCl buoyant density of 1.725 g $mL^{-1}$ and centrifuged in 5.1-mL Beckman polyallomer ultracentrifuge tubes in a Vti65.2 vertical rotor (Beckman

Coulter, Palo Alto, CA, USA) at 177000 × g for 44 h at 20 °C. DNA fractions with different densities were retrieved by displacing the gradient medium with sterile water from the top of the ultracentrifuge tube using an NE-1000 single-syringe pump (New Era Pump Systems Inc., Farmingdale, NY, USA) with a precisely controlled flow rate of 0.38 mL $min^{-1}$. Up to 15 gradient fractions were generated. The nucleic acids were separated from the CsCl by PEG 6000 precipitation, dissolved in 30 μL of TE buffer and stored at −20 °C (Jia and Conrad, 2009).

The abundances of bacterial and archaeal *amoA* genes and the comammox bacterial clade A *amoA* gene (because we observed only comammox clade A in the HL soil in this study) in the total DNA and fractionated DNA across the buoyant density gradients from DNA-SIP microcosms were analyzed as described above.

### 2.5. Phylogenetic analysis and access numbers of nucleotide sequences

Phylogenetic analysis of the comammox clade A *amoA* genes sequenced in this study was performed using the Molecular Evolutionary Genetics Analysis (MEGA 4.0) software package (Kumar et al., 2004). The basic tree of sequences from known comammox cultures and fosmid clones of the comammox *amoA* genes was constructed through a neighbor-joining tree using Kimura 2-parameter distance with 1,000 replicates to produce Bootstrap values.

The nucleotide sequences have been deposited in GenBank under the accession numbers listed in Table S2.

### 2.6. Statistic analysis

To determine the significance of the effects of soil type, fertilizer type and time evolution on $N_2O$ concentration, inorganic N concentrations and archaeal and bacterial *amoA* gene abundance, a three-way ANOVA analysis was conducted (Ho, 2006). The results were established in Supplementary Table S3. Multivariate analyses were conducted to measure the potential relationship between N dynamics ($N_2O$, $NH_4^+$ and $NO_3^-$) and nitrifiers abundance (AOA, AOB and comammox) (Figs. S3–S9, Table S4). All analyses were conducted using the SPSS 16.0 package for Windows (SPSS, Inc.), and $P < 0.05$ was considered to be statistically significant.

## 3. Results

### 3.1. Effects of NIs on $N_2O$ production

Urea amendment significantly stimulated $N_2O$ emissions in HL (Fig. 1A), JX (Fig. 1B), and SC (Fig. 1C) soil microcosms, and $N_2O$ emissions were inhibited by NI applications. The different patterns of total $N_2O$ emissions among the urea treatment and NI treatments were similar in the HL, JX and SC soils. The total $N_2O$ emissions in the urea treatments were significantly higher than those in the NI treatments ($P < 0.05$), while no significant difference was observed among the different NI treatments ($P > 0.05$). For each fertilizer treatment, no difference in the total $N_2O$ emission among different soils was observed in the control and NI treatments ($P > 0.05$). However, the total $N_2O$ emissions in the urea treatment were significantly higher in HL and SC than in JX ($P < 0.05$), while no difference was observed between HL and SC soils ($P > 0.05$).

In detail, the urea treatments exhibited significantly higher $N_2O$ emissions of 1274.8 (HL), 521.4 (JX) and 2503.1 (SC) ng $N_2O$-N $kg^{-1}h^{-1}$ at day 3 and 2746.6 (HL), 404.5 (JX) and 1414.8 (SC) ng $N_2O$-N $kg^{-1}h^{-1}$ at day 7 than the control and NI treatments ($P < 0.05$) (Fig. 1). At days 14 and 28, the $N_2O$ emission sharply decreased in the urea treatments in HL and SC, and no significant difference in $N_2O$ emission was observed in microcosms amended with NIs and urea ($P > 0.05$). In JX, $N_2O$ emissions remained higher in the urea treatments at days 14 and 28 than in the other treatments ($P < 0.05$). No significant difference was observed between NIs and control treatments in HL, JX and SC over time ($P > 0.05$), suggesting the effective inhibition of $N_2O$ emission by NIs in HL, JX and SC.

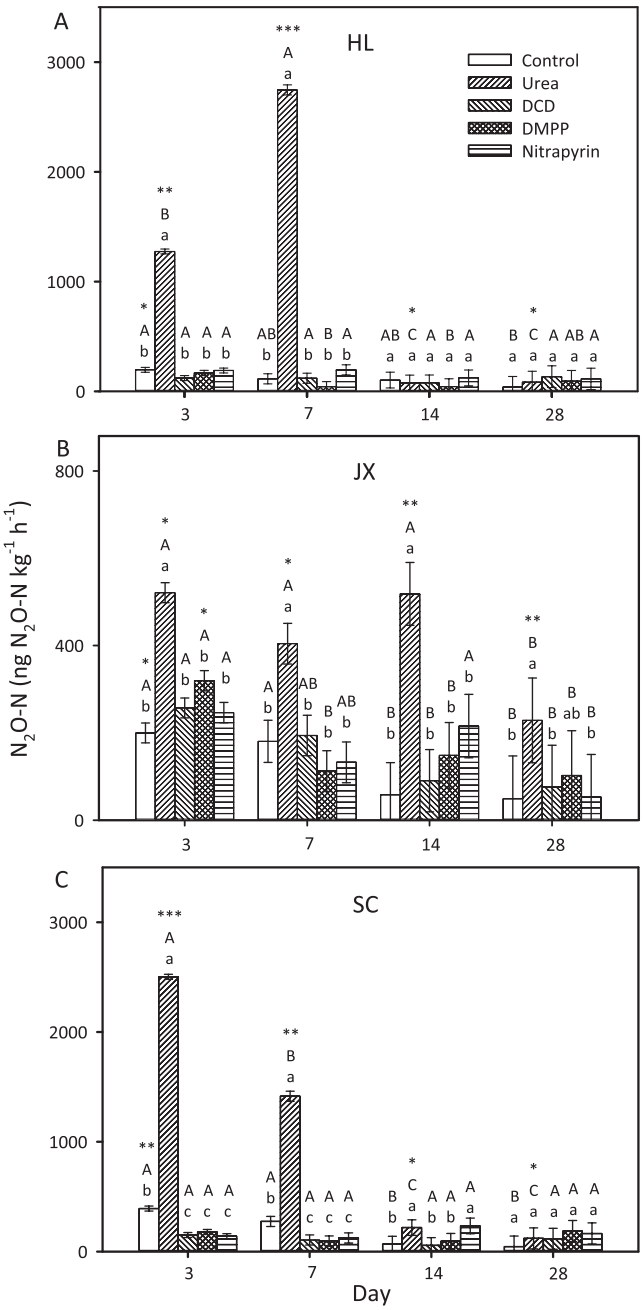


**Fig. 1.** Changes in $N_2O$ during incubation of soil microcosms for 3, 7, 14 and 28 days in HL (A), JX (B) and SC (C). Microcosms were amended with water only, urea, and urea with NIs (DCD, DMPP and nitrapyrin, respectively). $N_2O$ was analyzed before opening and $N_2O$ production rates were calculated as described in the Materials and Methods section. Mean concentration and standard errors of triplicate microcosms are presented. The different lowercase letter indicated the significant difference between different fertilizer treatments at each time point within the same soil; the different capital letters indicated the significant difference between each time point in the same fertilizer treatment within the same soil; the *, **, and *** indicated the difference between different soil in the same fertilizer treatment. The greater number of * indicated the significantly higher percentage change.

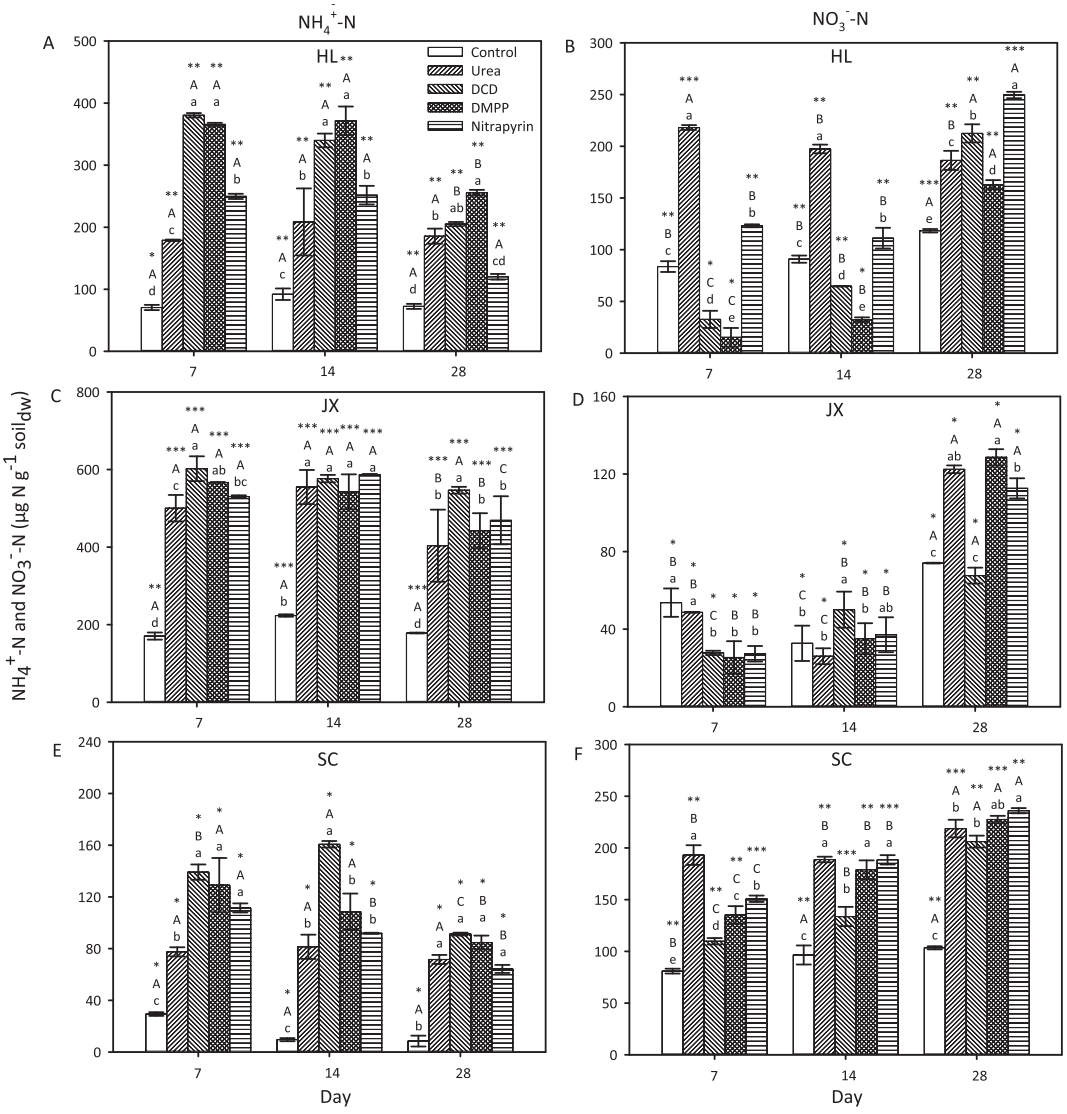


**Fig. 2.** Changes in $NH_4^+$-N (A, C, E) and $NO_3^-$-N (B, D, F) during incubation of soil microcosms for 7, 14 and 28 days in HL (A, B), JX (C, D) and SC (E, F). Microcosms were amended with water only, urea, and urea with NIs (DCD, DMPP and nitrapyrin, respectively). Concentration of $NH_4^+$-N and $NO_3^-$-N were determined after destructive sampling of triplicate microcosms. Mean concentration and standard errors of triplicate microcosms are presented. The different lowercase letter indicated the significant difference between different fertilizer treatments at each time point within the same soil; the different capital letters indicated the significant difference between each time point in the same fertilizer treatment within the same soil; the *, **, and *** indicated the difference between different soil in the same fertilizer treatment.

### 3.2. Effects of NIs on nitrification activity

In HL and SC, the change pattern of the inorganic N difference between urea and NI treatments was similar over time. The $NH_4^+$-N concentration in the urea treatments were significantly lower than that in the NI treatments at day 7 ($P < 0.05$) (Fig. 2A, 2E); however, no significant difference was detected between the urea and NI treatments at day 28 ($P > 0.05$). At each time point, no significant difference in $NH_4^+$-N concentration was observed in urea during microcosm incubation ($P > 0.05$), while a significant decrease in $NH_4^+$-N concentration was detected in NI treatments over time ($P < 0.05$). At day 28, the $NH_4^+$-N concentration in the urea treatment was equal to that in the DCD treatment, lower than that in the DMPP treatment, and higher than that in the nitrapyrin treatment of HL. There was no significant difference in $NH_4^+$-N concentration in urea and NI treatments of SC at day 28 ($P > 0.05$).

Consistent with the $NH_4^+$-N concentration results, the $NO_3^-$-N concentrations in the urea treatments were higher than those in the control treatments in HL and SC at day 28 ($P < 0.05$) (Fig. 2B, 2F), indicating that nitrification activity occurred in the urea-amendment treatments. In HL and SC, the $NO_3^-$-N concentration in urea treatments were significantly higher than those in NI treatments at day 7 ($P < 0.05$). At day 28, the $NO_3^-$-N concentration in urea treatment of HL was higher than that in DMPP of HL, while the $NO_3^-$-N concentration in urea was equal or lower than those in the other NI treatments in HL and SC.

In JX, no significant difference in the $NH_4^+$-N concentration was observed in the urea and nitrapyrin at day 7 ($P > 0.05$), and the $NH_4^+$-N concentration in urea was lower than those in DCD and DMPP treatments ($P < 0.05$) (Fig. 2C). At day 28, no statistically significant difference in $NH_4^+$-N concentration was detected between urea, DCD and DMPP treatments ($P > 0.05$), while the $NH_4^+$-N concentration in DCD was significantly higher than those in urea, DMPP and nitrapyrin treatments ($P < 0.05$). During time evolution, the $NH_4^+$-N concentration in urea, DMPP and nitrapyrin decreased during incubation ($P < 0.05$), whereas the $NH_4^+$-N concentration did not change during the incubation in DCD treatment ($P > 0.05$). The $NO_3^-$-N concentration in urea was significantly higher than those in NIs treatments

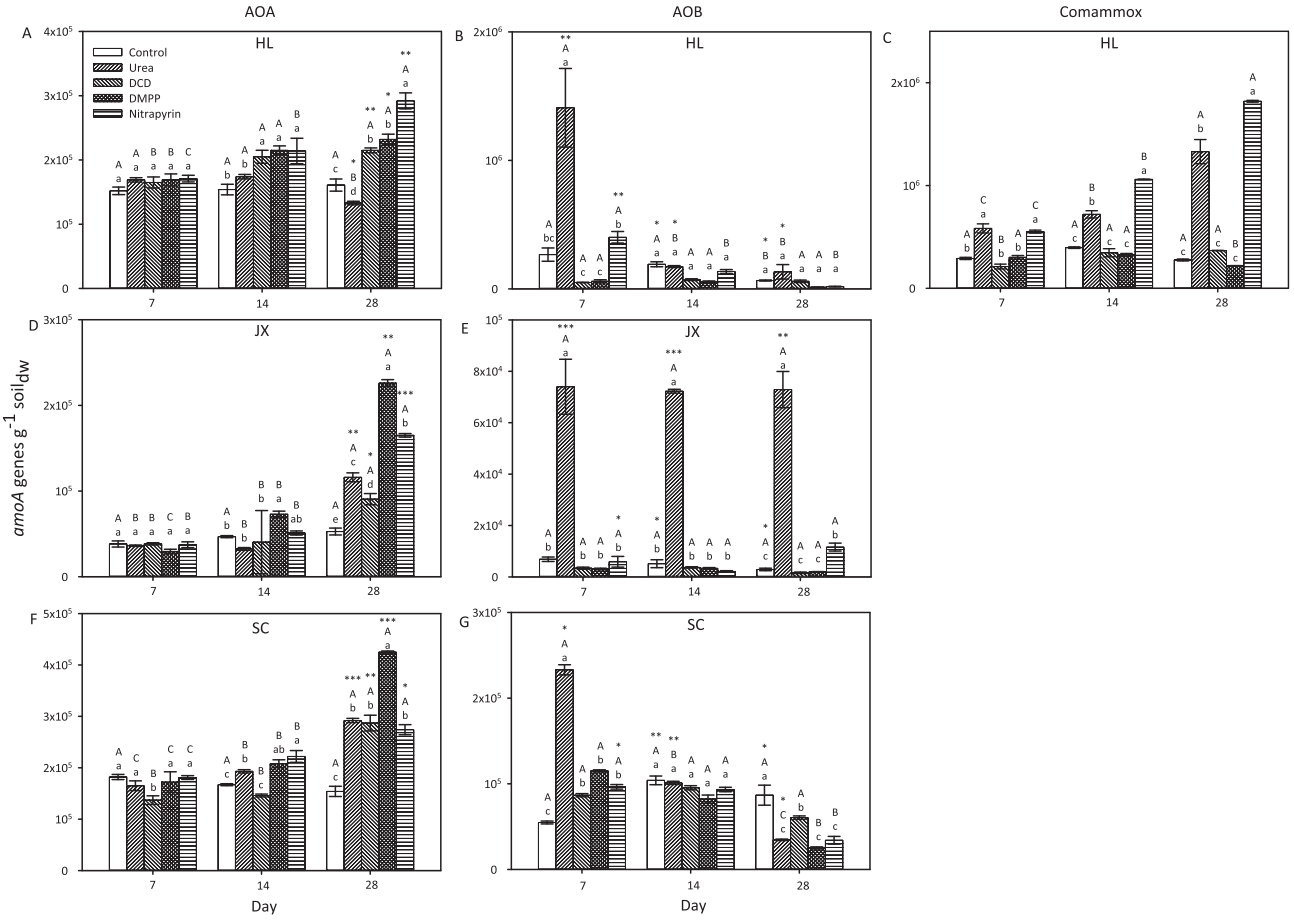


**Fig. 3.** Changes in the abundance of archaeal (A, D, F), bacterial (B, E, G) and comammox (C) *amoA* genes during incubation of HL (A, B, C), JX (D, E) and SC (F, G) soil microcosms. Quantitation was performed from destructively sampled soil microcosms incubated for 7, 14 and 28 days that were amended with water only, urea, and urea with NIs (DCD, DMPP and nitrapyrin, respectively). Mean concentration and standard errors of triplicate microcosms are presented. The different lowercase letter indicated the significant difference between different fertilizer treatments at each time point within the same soil; the different capital letters indicated the significant difference between each time point in the same fertilizer treatment within the same soil; the *, **, and *** indicated the difference between different soil in the same fertilizer treatment.

at day7 ($P < 0.05$) (Fig. 2D). However, the $NO_3^-$-N concentration in urea treatment decreased at day 14 ($P < 0.05$). The $NO_3^-$-N concentration in all the treatment increased at day 28 ($P < 0.05$). At day 28, the $NO_3^-$-N concentration in urea was equal to those in DMPP and nitrapyrin treatments ($P > 0.05$), whereas it was significantly higher than that in DCD treatment ($P < 0.05$).

In the same fertilizer treatment at the same time point, the $NH_4^+$-N concentrations were higher in JX (labeled with *** in Fig. 2C) than those in HL and SC ($P < 0.05$). However, the $NO_3^-$-N concentration was lower in JX (labeled with * in Fig. 2D) than those in HL and SC ($P < 0.05$).

### 3.3. Effect of NIs on AOA, AOB and comammox amoA genes

For each soil type, the difference in AOA abundance among each treatment during time evolution was similar (Fig. 3A, 3D, 3F). Compared with the AOA abundance in the control and NI treatments, no significant increase in AOA abundance in the urea treatment was detected at day 7 in HL, JX and SC, respectively ($P > 0.05$). The higher AOA abundance in the urea treatment at day 28 was only observed in JX and SC compared to that in the control treatment ($P < 0.05$). At day 28, the AOA abundance in the urea treatment was equal to or lower than that in NI amendment treatments in each soil, except DCD in the JX soil. During incubation time evolution, the AOA abundance significantly increased in the urea treatment of JX and SC and in the NI treatments of HL, JX and SC ($P < 0.05$). For each fertilizer treatment, we calculated the percentage change ((AOA copy number at day 7, 14 or 28 – AOA copy number at day 0)/AOA copy number at day 0) to compare the change pattern of AOA between different soil types. In each treatment, a significant difference in AOA percentage change among different soils was only observed at day 28 ($P < 0.05$).

The AOB abundance in the urea treatments at day 7 were significantly higher than those in the control treatment of HL, JX and SC ($P < 0.05$), respectively, suggesting that urea amendment stimulated AOB growth (Fig. 3B, 3E, 3F). For each soil, the difference in AOB abundance between the urea and NI treatments during the time evolution was similar in HL and SC; AOB abundance in the urea treatments were significantly higher than that in the NI treatments at day 7 ($P < 0.05$); the AOB abundance sharply decreased at day 14 ($P < 0.05$) and remained stable at day 28. In JX, the AOB abundance in urea was significantly higher than those in NI treatments at day 7, day 14 and day 28 ($P < 0.05$), respectively. During time evolution, the AOB abundance in the urea treatment remained unchanged during incubation ($P > 0.05$). There was no significant increase in AOB abundance in the NI treatments during incubation ($P > 0.05$). Unlike the results of AOA abundance, a significant difference in AOB percentage change among difference soil types were mainly observed in urea treatments at each time point ($P < 0.05$). The AOB percentage change in the urea treatment of JX was higher than those in HL and SC ($P < 0.05$).

The comammox clade A *amoA* gene was detected in HL, as confirmed by PCR amplicon-agarose gel electrophoresis and cloning (Fig.

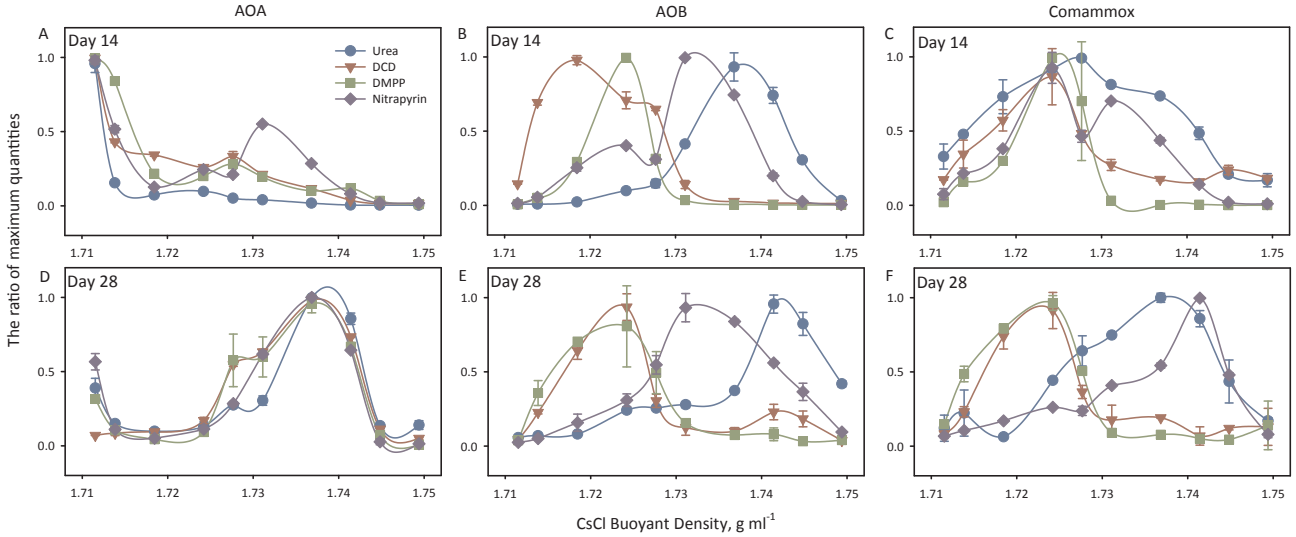


**Fig. 4.** Quantitative distribution of the relative abundance of the AOA (A, D), AOB (B, E) and comammox (C, F) *amoA* genes retrieved from different treatments ($^{13}CO_2$ + Urea, $^{13}CO_2$ + Urea + DCD, $^{13}CO_2$ + Urea + DMPP, and $^{13}CO_2$ + Urea + Nitrapyrin) in the 14-day (A, B, C) and 28-day (D, E, F) DNA-SIP microcosms of the HL soil. Error bars represent standard errors from three replicates.

S1). The comammox abundance in urea and nitrapyrin were significantly higher than those in other treatments at day 7, 14 and 28 ($P < 0.05$), respectively (Fig. 3C). The comammox abundance kept increasing from day 7 to day 28 ($P < 0.05$). At day 14 and day 28, the comammox abundance in the nitrapyrin treatment was higher than that in the urea treatment ($P < 0.05$).

Pearson correlation analysis between N dynamics ($N_2O$, $NH_4^+$-N and $NO_3^-$-N) and microbial abundance (AOA, AOB and comammox) showed the potential contribution of microbes to N conversion (Figs. S3–S9, Table S4). The AOA abundance increased and $NH_4^+$-N concentration decline during incubation in DCD treatment of HL (Fig. S3), DMPP treatment of JX (Fig. S6) and DMPP and nitrapyrin treatments of SC (Fig. S8). Meanwhile, the population size of AOA and $NO_3^-$-N concentration both increased during incubation in DCD and DMPP treatments of HL (Fig. S3), DCD, DMPP and nitrapyrin treatments of both JX (Fig. S6) and SC (Fig. S8). The AOB abundance and $N_2O$ emission both decline during incubation in HL (Fig. S4) and SC (Fig. S9) and remained stable with the unchanged $N_2O$ emission in JX. The comammox abundance increased and $NH_4^+$-N concentration and $NO_3^-$-N concentration decreased and increase during incubation in DCD of HL, respectively (Fig. S5). It should be notable that most of the *P* values according to Pearson correlation analysis were larger than 0.05, suggesting no significant correlation, which might be due to only three points were measured during each Pearson correlation analysis.

### 3.4. $N_2O$ production and nitrification activity during DNA-SIP microcosm incubation

In the HL DNA-SIP microcosm (Fig. S10A), the $N_2O$ emission rate from the urea treatment was 3335.1 ng $N_2O$-N $kg^{-1}$ at day 7, which was significantly higher than the $N_2O$ emission amount of the other treatments ($P < 0.05$). $N_2O$ emission from the urea treatment decreased sharply at day 14 ($P < 0.05$) and continued to decrease to an amount as low as that from the other treatments. In addition, no significant changes were observed among all the treatments at day 28 ($P > 0.05$). In the JX DNA-SIP microcosm (Fig. S10B), the $N_2O$ emissions from the urea (1315.6 ng $N_2O$-N $kg^{-1}$) and nitrapyrin (1206.7 ng $N_2O$-N $kg^{-1}$) treatments were significantly ($P < 0.05$) higher than those from the DCD (557.3 ng $N_2O$-N $kg^{-1}$) and DMPP (871.5 ng $N_2O$-N $kg^{-1}$) treatments at day 7 ($P < 0.05$). At day 14, day 21 and day 28, the $N_2O$ emissions from the urea of JX were higher than those in other NI treatments ($P < 0.05$).

### 3.5. Dynamics of AOA, AOB and Nitrospira amoA genes during DNA-SIP microcosm incubation

In the DNA-SIP microcosms of HL (Fig. S11A, S11B, and S11C), no significant differences in AOA *amoA* gene abundance were observed among treatments at day 14 ($P > 0.05$), whereas the AOA *amoA* gene abundance was greater in the NIs-amended soil microcosms at day 28 than in the urea-amended soil microcosms ($P < 0.05$). The AOB abundance in the urea-amended treatment was significantly higher than that in the NI-amended treatments at day 14 ($P < 0.05$). At day 28, the copy number of the AOB *amoA* gene in the urea-amended treatment remained stable, whereas the AOB abundance in the nitrapyrin-amended treatment increased. The abundance of the comammox clade A *amoA* gene in urea and nitrapyrin treatments were significantly higher than those in DCD and DMPP at day 14 and day 28, respectively ($P < 0.05$). Significant increases in comammox clade A abundance were detected in the urea- and nitrapyrin-amended microcosms at day 28 ($P < 0.05$), whereas no significant change was observed in the DCD- and DMPP-amended microcosms between day 14 and day28 ($P > 0.05$).

In the DNA-SIP microcosm of JX (Fig. S11D, S11E), no significant differences in AOA *amoA* gene abundance were observed among the treatments at day 14 ($P > 0.05$), while the AOA *amoA* gene abundance significantly increased in the urea- and DMPP-amended microcosms compared to the other microcosms at day 28 ($P < 0.05$), in which the abundance remained stable during incubation ($P > 0.05$). The AOB abundance in the urea-amended treatment was significantly higher than those in the NI-amended treatments at both day 14 and day 28 ($P < 0.05$).

### 3.6. DNA-SIP analysis of the AOA, AOB and comammox amoA genes associated with nitrification

The Fig. 4 shows the SIP profiles of AOA, and comammox clade A *amoA* genes in HL during DNA-SIP microcosm incubation. At day 14, the AOA *amoA* gene in the urea-amended treatment and the comammox clade A *amoA* genes in the urea- and nitrapyrin-amended treatments exhibited partial shifts toward high densities, and the AOB *amoA* gene in the urea- and nitrapyrin-amended treatments was greatly enriched in the fractions with high densities. At day 28, the AOA *amoA* genes in all the treatments were enriched at high densities, and the comammox clade A *amoA* genes in the urea and nitrapyrin treatments were greatly

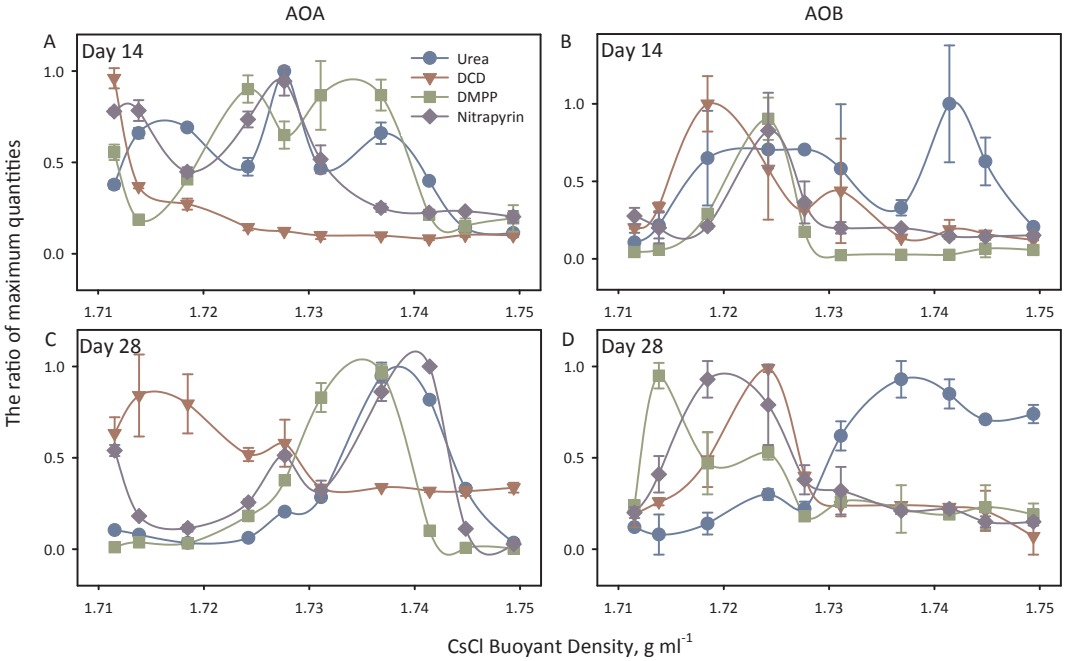


**Fig. 5.** Quantitative distribution of the relative abundance of the AOA (A, C) and AOB (B, D) *amoA* genes retrieved from different treatments ($^{13}CO_2$ + Urea, $^{13}CO_2$ + Urea + DCD, $^{13}CO_2$ + Urea + DMPP, and $^{13}CO_2$ + Urea + Nitrapyrin) in the 14-day (A, B) and 28-day (C, D) DNA-SIP microcosms of the JX soil. Error bars represent standard errors from three replicates.

enriched in fractions with high densities. Similar to the results at day 28, the AOB *amoA* genes were significantly enriched in the heavy DNA fractions in the urea- and nitrapyrin-amended treatments.

In the DNA-SIP microcosm of JX (Fig. 5), the AOA *amoA* genes in the urea-, DMPP- and nitrapyrin-amended treatments exhibited a partial shift in fractions with high densities at day 14 and were further greatly enriched in the high-density fractions at day 28. In contrast to the NI-amended treatments, the urea-amended treatment harbored AOB communities enriched in the heavy SIP fractions at only day 14 and day 28.

## 4. Discussion

### 4.1. Effective inhibition of NIs on AOB rather than AOA or AOA-driven nitrification process

In each soil, urea application stimulated the nitrification process in the absence of NIs. However, nitrification rates evolved differently during incubation: the $NO_3^-$-N concentration significantly increased at day 7 in HL and SC (accounting for 100% and 82.4% of the total increase $NO_3^-$-N, respectively) and slightly changed during the rest of the incubation period (Fig. 2B, 2F), while the $NO_3^-$-N concentration in JX mainly increased at days 15–28 (accounting for 89.0% of the total increase $NO_3^-$-N in JX) (Fig. 2D). Moreover, the total $NO_3^-$-N increase amounts in HL (156.5 μg N $g^{-1}$ $soil_{dw}$) and SC (145.8 μg N $g^{-1}$ $soil_{dw}$) were significantly higher than that in JX (108.3 μg N $g^{-1}$ $soil_{dw}$). Soil pH has been reported as a major factor regulating the nitrification process in soil, that nitrification is rapid in soils with pH > 6.0 (Sahrawat, 2008). Moreover, the differentiation in the increasing pattern of the $NO_3^-$-N concentration might be the result of niche differentiation of active ammonia oxidizers among these soils. The AOB abundance rather than AOA significantly increased at day 7 in both HL (Fig. 3B) and SC (Fig. 3G), which agreed with the significant $NO_3^-$-N increase at day 7. In JX, although the AOB abundance increased at day 7 (Fig. 3E), the *in situ* AOA abundance was much higher than AOB and increased during days 15–28, accompanied with significant $NO_3^-$-N increase (Fig. 3D), suggesting the dominant contribution of AOA to the nitrification process in JX. Soil pH might be the key factor that governs the differentiation of active ammonia oxidizers in this study: AOB controls ammonia oxidization in alkaline soils (Shen et al., 2008), while AOA has a competitive advantage in acidic soils (Jiang et al., 2015; Zhang et al., 2012). Moreover, the activity of AOB was also observed in JX, where the increase AOB abundance (Fig. 3E) and the enrichment of $^{13}C$-labeled AOB were observed during incubation (Fig. 5). These results might be due to the high N amendment in acidic soils (Huang et al., 2018; Wu et al., 2011). In addition, the lower abundance of AOA and AOB in JX than those in HL and SC might also contribute to the lower nitrification activity in JX. The initial $NH_4^+$-N concentration was higher in JX, the possible explanation led to the higher $NH_4^+$-N in JX was the higher mineralized N in JX. For example, although we added 200 ppm urea-N, approximately $NH_4^+$ increased by approximately 338.4 ppm in urea-amended treatments in JX, which might come from the mineralization of native organic N (Hirzel et al., 2012).

Although AOA did not increase in the urea treatment of HL soil during incubation, $^{13}C$-labeled AOA was observed in the heavy fractions, identifying the potential activity of AOA. This result suggested the advantage of the DNA-SIP technique to reveal the activity of microbes, especially when some phylotypes of functional microbes decreased during incubation, which could not reflect the increase in the abundance of functional microbes when only measuring the total abundance of functional microbes through quantitative PCR.

The comammox bacteria was detected in only HL in this study, and urea application significantly increased the comammox population (Fig. 3C). In addition, comammox incorporated $^{13}C$-$CO_2$ into their genomes during incubation (Fig. 4), suggesting the activity of comammox. Recent studies provided evidence that comammox clade A played a potential role in nitrification of agricultural soils (Li et al., 2019a), whereas comammox clade B was linked with the nitrification process in the absence of $NH_4^+$-N amendment (Wang et al., 2019). Our study confirmed the activity of comammox clade A in agricultural soils with N amendment (Fig. S2). Li et al. (2019a), Li et al. (2019b) showed the $^{13}C$-labelled comammox Nitrospira belong to Cluster 1 and 2 of clade A (Li et al., 2019a). Our study demonstrated the activity of comammox Nitrospira fell within Cluster 1, which has been observed from

various ecosystems. Additionally, the sequences of comammox Nitrospira *amoA* genes in this study could be divided into Cluster 1.1 and 1.2. Four out of eleven comammox clones was phylogenetically close to the sequences detected in (Li et al., 2019a), belong to Cluster 1.1, while other clones (seven out of eleven) fell into Cluster 1.2. Oligotrophic conditions have also been supposed to be an ideal ecological niche for comammox (Costa et al., 2006; Kits et al., 2017; van Kessel et al., 2015), especially in water engineering ecosystems (Bartelme et al., 2017; Fowler et al., 2018; Palomo et al., 2016; Palomo et al., 2018; Pinto et al., 2016; Pjevac et al., 2017; Wang et al., 2017b; Xia et al., 2018). The recent study (Li et al., 2019a) and our study both demonstrated the activity of comammox in the soils with intense N fertilization, suggesting that comammox might adapt to broader substrate concentrations than previously thought.

No detectable $NO_3^-$-N increase was observed at day 14 and day 28 in the urea treatment of HL, which was not consistent with the activity of AOA and comammox observed at day 28. We assumed two possible explanations. First, $NO_3^-$-N, produced by AOA and comammox, was consumed by heterotrophic denitrification (Chen and Ni, 2012), which might partly be due to the high organic matter in HL. Second, an unidentified energy source rather than $NH_3$ oxidation might support the growth of AOA and comammox. Further research is indeed needed to test this hypothesis.

Compared to urea treatment, NI amendment delayed the nitrification process rather than migrating it, regardless of soil type and NI type. In HL and SC, the $NO_3^-$-N concentration in NI amendment treatments were significantly lower than that in urea treatment at day 7 and day 14 (Fig. 2B, 2F), which might be attributed to the effective inhibition of the growth and metabolic activity of AOB by NIs (Fig. 3B, 3G). The increasing $NO_3^-$-N concentration in the NI treatments was detected at day 28 (Fig. 2B, 2F), consistent with the growth of AOA at day 28 in HL and SC (Figs. 3A, 3F, S3, S8). Although AOB had a lower abundance than AOA in acidic soil (JX), NIs still successfully inhibited the activity of AOB rather than AOA. Taken together, our results demonstrated the inhibition of AOB activity and AOB-driven nitrification by NIs in most of the soil microcosms (except for the successful inhibition of both AOA and AOB by DCD in JX soil). Moreover, we identified the increase of AOA abundance and the enrichment of $^{13}$C-labeled AOA in the heavy fractions in the NI treatment (except in the DCD treatment of JX) that linked with the increase of $NO_3^-$-N, suggesting the low or null efficacy of NIs on AOA. These results therefore demonstrated the important role of NIs in minimizing fertilizer loss by inhibiting the growth and activity of AOB, which agrees well with the results of previous studies that the inhibitory effects of DCD, DMPP and nitrapyrin on AOB but not AOA in soils with different properties (Chen et al., 2019; Di and Cameron, 2011; Fan et al., 2019; Florio et al., 2014; Fu et al., 2018; Gong et al., 2013; Kleineidam et al., 2011; Lan et al., 2018; Shi et al., 2016a; Shi et al., 2016b). Thus, we assumed that NIs have selective inhibitory effects on ammonia oxidizers and that they inhibited AOB rather than AOA. DCD, DMPP and nitrapyrin have been previously shown to have little effect on AOA pure culture (Shen et al., 2013) and in laboratory microcosm incubation (Shi et al., 2016a; Shi et al., 2016b). The different susceptibilities on AOA and AOB might be attributed to the fundamental differences in the cellular structure and the $NH_3$ oxidation pathways of AOA and AOB. The DCD, DMPP and nitrapyrin are suggested to act as metal chelators by binding copper in the active site of the amoB subunit (McCarty, 1999; Ruser and Schulz, 2015). For AOB, periplasmic amoB presumably contains an active site that catalyzes reactions using copper (Balasubramanian et al., 2010), whereas activity assays of isolated archaeal amoB indicate an inactive enzyme (Lawton et al., 2014), and amoC or the amoX subunit might serve as the active site for AOA (Tolar et al., 2017).

Although AOB has been reported to be more competitive under the high substrate environment than AOA (Verhamme et al., 2011), we identified the ability of AOA to grow at high $NH_4^+$ concentrations in NIs treatments with the absence of AOB activity, which agreed well with the results of previous investigations established in (Chen et al., 2019; Chen et al., 2015; Fan et al., 2019; Hink et al., 2018). We hypothesized that there might be two explanations for this result. First, in some NI treatments (DCD, DMPP and nitrapyrin treatments of HL, DMPP and nitrapyrin treatments of JX and DMPP treatment of SC), the AOA abundance was higher than that of urea-amended treatments (Fig. 3). These results suggested that NIs might act as carbon substrates and stimulate AOA growth. Second, as AOA and AOB use the same substrate for growth and exhibit different cellular biochemistry and physiology, they have different relative competitiveness under conditions with distinct characteristics. Our results suggest that AOA could be more competitive because the activity of their competition AOB was suppressed.

Our study also demonstrated that the efficacy of NIs is dependent on soil chemical properties. For example, compared with the DCD and DMPP treatments in this study, lower effective efficacy on AOB was detected in nitrapyrin of HL soil at day 7 (Fig. 3B). There were two possible explanations. First, nitrapyrin concentration was lower than DCD and DMPP, which might not completely diffuse in soils at day 7; second, the high soil organic matter in HL might also result in a high adsorption rate of nitrapyrin and therefore low availability. In longer incubation studies, it has been demonstrated that adsorption led to a decrease in the efficiency of the nitrapyrin with organic matter content (Hendrickson and Keeney, 1979). Moreover, the comammox abundance in nitrapyrin was even higher than that in urea treatment. We assumed that nitrapyrin or its mineralized production might stimulate the growth of comammox. To understand the inhibitory mechanism of nitrapyrin, future experiments conducted with $^{14}$C-labeled nitrapyrin might be taken into consideration to identify the relative rates of mineralization, absorption or other physical biochemical processes. In the acidic JX soil, DCD effectively inhibited the activity of AOA (Fig. 5). This result was consistent with the previous literature that reported the effective inhibition of the growth and activity of AOA in acidic soils by DCD (Zhang et al., 2012). Guardia et al. (2018) showed the effective inhibition of DCD on the acid soil with the lowest CEC, suggested the soils with low pH and relatively low CEC was a suitable environment for DCD (Guardia et al., 2018), which might be the reason of the efficacy DCD in JX of this study. However, the investigation also reported the high efficacy of DMPP (Guardia et al., 2018), which was inconsistent with the result of this study. The opposite results implied multiple soil physio-chemical properties potentially affect the efficacy of NIs together. Moreover, although AOA did not assimilate $^{13}CO_2$ in DCD treatment of JX, the growth of AOA was observed (Fig. 2D), which might be attributed to mixotrophic growth of AOA (Tourna et al., 2011).

### 4.2. Efficiency inhibition of NIs on $N_2O$ production

The effect of NIs on the $N_2O$ production has been reported to be influenced by many environmental factors, such as soil pH (Shi et al., 2016a; Shi et al., 2016b; Wang et al., 2017a), soil moisture (Di et al., 2014) and soil temperature (Menéndez et al., 2012). Because of the stable soil moisture and incubation temperature in this study, we mainly discussed the influence of soil pH on the efficacy of NIs on the $N_2O$ emission. The $N_2O$ emission and AOB abundance had the same change pattern in urea treatment of both HL and SC (Figs. S4, S9), suggesting the potentially direct or indirect contribution of AOB in $N_2O$ emission. Compared with the $N_2O$ emissions in the urea treatments, significantly lower $N_2O$ emissions were established in NI amended treatments (Fig. 1A, 1C), accompanied with the inhibition of AOB, suggesting the effective inhibition of $N_2O$ emissions by NIs. This finding was corroborated in previous studies, which have found a great contribution of NIs to $N_2O$ inhibition (Cassman et al., 2019; Chen et al., 2019; Dai et al., 2013; Fan et al., 2019; Gilsanz et al., 2016; Li et al., 2019b; Misselbrook et al., 2014; Soares et al., 2016; Wang et al., 2017a). Thus, our result further suggested that NIs inhibited $N_2O$

production by migrating $NH_4^+$ oxidation through suppressing AOB activity (Müller et al., 2002; Zerulla et al., 2001). Previous studies have demonstrated that the nitrification and nitrifier-induced denitrification were dominant pathways of $N_2O$ production by AOB in alkaline soils (Shaw et al., 2006; Shi et al., 2017), which might be the predominant pathway of $N_2O$ emission in HL and SC.

In JX, although the $N_2O$ emission was higher in the urea treatment than those in the other treatments (Fig. 1B), no significant increase of $NO_3^-$-N was detected in the urea treatment from day 7 to 14, and it even decreased (Fig. 2D), suggesting that denitrification might occur in JX. Although it has been concluded that the optimum pH for the majority of denitrifiers in culture medium is between 7 and 8, the optimum pH for denitrification might be broader (ŠImek and Cooper, 2002). For example, heterotrophic denitrification has been demonstrated as the main pathway for $N_2O$ emission in acidic soils (Shi et al., 2017). However, although we assumed that the denitrification process might occur in urea treatment of JX, the relative contributions of multiple biological pathways to $N_2O$ production could not be clarified in this study. Further work using a dual-isotope ($^{18}O$- $^{15}N$) labeling technique (Kool et al., 2011; Kool et al., 2010; Shi et al., 2017) might be available to identify the differentiation in $N_2O$ production pathways in these soils. It should be noted that the dominance of heterotrophic denitrification was observed in acidic soils, which were dominated by AOA (Shi et al., 2017). However, AOA and AOB were both active in JX soil. Considering the effective inhibition of AOB growth and activity and $N_2O$ emission, we assumed that nitrification and nitrifier-induced denitrification driven by AOB also contributed to $N_2O$ production in JX and this process was successfully inhibited by NIs application.

Although NIs effectively inhibited the $N_2O$ emission mainly by migrating AOB activity, the contribution of denitrification to $N_2O$ emission could not be neglected. It has been reported that the different $N_2O$ emission pathway in the soils with different pH was mainly attributed to the different active ammonia oxidizers, which harbor distinct $N_2O$ emission pathways. It is notable that pH not only influence the $N_2O$ emission by influencing the active ammonia oxidizers, but also influence the end product of denitrification. For example, previous study reported that at lower soil pH, denitrification yields relatively more $N_2O$ leading to a greater $N_2O/N_2$ ratio (ŠImek and Cooper, 2002), which may also contribute to the importance of heterotrophic denitrification pathway in $N_2O$ production in acidic soils. Application of $NH_4^+$-based fertilizers could lead to further soil acidification (Bolan et al., 1991; He et al., 2012), which would increase the importance of heterotrophic denitrification in $N_2O$ emission. Thus, future work regarding the effect of NIs on denitrification process and product is needed.

The increase of $NO_3^-$-N concentration and AOA abundance were observed at the end of incubation in most of the NI treatments in this study. However, no significant $N_2O$ emission was detected. This result might be explained by the previous reports, in which AOB rather than AOA was widely linked with $N_2O$ emissions (Cassman et al., 2019; Dai et al., 2013; Di and Cameron, 2011; Meinhardt et al., 2018; Soares et al., 2016; Wang et al., 2016a; Wang et al., 2016b). A large number of studies debated the effect of NIs on denitrifiers abundance. For example, the application of NIs with urea decreased the abundance of *nirS* gene (encoded nitrite reductase enzyme) (Dong et al., 2013b), *nirK* gene (encoded nitrite reductase enzyme) and *nosZ* gene (encoded nitrous oxide reductase enzyme) (Florio et al., 2014), while in other studies DPPM did not influence the *narG* (encoded $NO_3^-$ reductase enzyme), *nirK* and *nosZ* gene abundances (Dong et al., 2018; Duan et al., 2017; Huang et al., 2014; Kou et al., 2015; Shi et al., 2016b). Barrena et al. showed that soil moisture, which linked with the oxygen concentration, influenced the effect of NIs denitrifying gene, that under 40% of soil water filled pore space (WFPS), the application of DMPP significantly decrease of the *narG*, *nirK* and *nosZ* gene abundances also decreased, while the application of DMPP did not decrease the denitrifying gene abundances (narG, nirK and nosZ) under 80% of WFPS (Barrena et al., 2017). The WFPS was 50% in this study. Therefore, we assumed that NIs might effective in migrating heterotrophic denitrification by inhibiting denitrifying genes in this study. However, the change pattern of the abundance of key genes encoding denitrification could not reflect the NIs directly inhibited the genes or indirectly inhibited. In fact, isotopic analysis showed that nitrification inhibitors have no direct effect on denitrification and indirectly inhibit denitrification due to the reduced substrate (nitrate) delivery to microsites where denitrification occurs (Wu et al., 2017; Wu et al., 2018). Moreover, Wu et al. demonstrated that NI could increase $N_2$ production and reduce $N_2O/N_2$, which might be another possible explanation for the results in JX (Wu et al., 2018). More work in the further is needed to clarify the effect of NIs on denitrifiers.

The comammox was also not responsible for $N_2O$ production in the HL soil, as no increase in $N_2O$ emission was linked to the increase of the comammox *amoA* gene during the incubation, which might be due to the lack of homologs of AOB NO reductase genes (Daims et al., 2015; Kits et al., 2017).

### 4.3. Limitations and future work

(1) Other factors may also contribute to the efficacy of NIs, such as soil temperature, soil properties, moisture, and timing of application (Di and Cameron, 2018; Di et al., 2014; Florio et al., 2016; Guardia et al., 2018; Lan et al., 2018). Therefore, these factors should be taken into consideration to better understand the efficacy of NIs in future studies.
(2) The sample collection frequency was not enough to accurately establish the nitrification dynamics in this study, as soil $NH_4^+$-N and $NO_3^-$-N were measured only three times (days 7, 14 and 28), but day 3 was key for $N_2O$ losses. Future work should increase the sample collection frequency.
(3) Measuring the total nitrogen (TN) concentrations might help to quantify the ammonia loss due to ammonia volatilization during the experiment in the future study.
(4) Field work. We should note that there might be a significant difference of the results between laboratory research and field work. Plant growth would affect nutrient availability and soil properties, which consequently influences the effects of NIs. Thus, future work might focus on the effects of NIs in the field.
(5) Although the efficiency of NIs has been widely identified, the use of nitrification inhibitors also increases cost, potential for $NH_3$ emission and the risk of environmental contamination (Qiao et al., 2015), for example nitrapyrin has been detected in streams (Woodward et al., 2016), and DCD residues were detected in milk as a result of DCD use in pastures (Thapa et al., 2016). Thus, the efficacy of environmentally friendly biological nitrification inhibition (BNI) on N dynamics and microbes requires future investigation.
(6) At day 14 and 28, the stable $NH_4^+$ concentration in the urea treatments of HL was still high, suggesting that the nitrification was not very intense in this experiment. Moreover, the N supply in this study is very high (500–568 kg N/ha), which might stimulate different ammonia oxidizers compared with those in relatively low N supply soils. Thus, different substrate concentrations should be taken into consideration when considering the efficiency of NIs in the future study.

## 5. Conclusion

In summary, the NIs in our experiment were revealed to target $N_2O$-producing AOB in soils and have a substantial impact on mitigating $N_2O$ emissions. However, the increase of $NO_3^-$-N was not inhibited and was linked with the increase in non-$N_2O$-producing AOA. Our results supported the hypothesis that NIs have a selective effect on AOB than AOA. Furthermore, we provided evidence that comammox contributed to the

nitrification process without producing $N_2O$. DCD and DMPP rather than nitrapyrin effectively inhibited comammox increase and activity. The efficacy of NIs was also dependent on soil chemical properties, that nitrapyrin did not inhibit AOB growth at the beginning of microcosm incubation in the HL soil, while DCD successfully inhibited the increase of both AOA and AOB in the JX soil. Further studies involving more soil types under field conditions should be incorporated into research regarding the efficacy of NIs at inhibiting nitrification and nitrifier activity. Moreover, although many studies have targeted on the effects of NIs on the abundance, community composition and activity of nitrifying guilds, the precise mechanism of these effects has not yet been clarified. We think that stable isotope labeled NIs amended microcosm incubation might be a good method for further study of the effect mechanisms of NIs.

## Declaration of Competing Interest

The authors declare that they have no known competing financial interests or personal relationships that could have appeared to influence the work reported in this paper.

## Acknowledgement

X. Zhou acknowledges financial support from the National Natural Science Foundation of China (41807029) and Fundamental Research Funds for the Central Universities (B200201028). C. Lu acknowledges financial support from the National Natural Science Foundation of China (51679067 and 51879088), and Fundamental Research Funds for the Central Universities (B200204002). The authors are very grateful for helpful comments from reviewers and editors.

## Appendix A. Supplementary data

Supplementary data to this article can be found online at https://doi.org/10.1016/j.geoderma.2020.114637.

## References

Balasubramanian, R., et al., 2010. Oxidation of methane by a biological dicopper centre. Nature. 465 (7294), 115–131.
Barrena, I., et al., 2017. Soil water content modulates the effect of the nitrification inhibitor 3, 4-dimethylpyrazole phosphate (DMPP) on nitrifying and denitrifying bacteria. Geoderma. 303, 1–8.
Bartelme, R.P., et al., 2017. Freshwater Recirculating Aquaculture System Operations Drive Biofilter Bacterial Community Shifts around a Stable Nitrifying Consortium of Ammonia-Oxidizing Archaea and Comammox Nitrospira. Front. Microbiol. 8, 101.
Bolan, N.S., et al., 1991. Processes of soil acidification during nitrogen cycling with emphasis on legume based pastures. Plant and Soil. 134 (1), 53–63.
Cassman, N.A., et al., 2019. Nitrification inhibitors effectively target N2O-producing Nitrosospira spp. in tropical soil. Environ. Microbiol. 21 (4), 1241–1254.
Chen, H., et al., 2019. Reduction of N2O emission by biochar and/or 3,4-dimethylpyrazole phosphate (DMPP) is closely linked to soil ammonia oxidizing bacteria and nosZI-N2O reducer populations. Sci. Total Environ. 694, 133658.
Chen, Q., Ni, J., 2012. Ammonium removal by Agrobacterium sp. LAD9 capable of heterotrophic nitrification–aerobic denitrification. J. Biosci. Bioeng. 113 (5), 619–623.
Chen, Q.H., et al., 2015. Comparative effects of 3,4-dimethylpyrazole phosphate (DMPP) and dicyandiamide (DCD) on ammonia-oxidizing bacteria and archaea in a vegetable soil. Appl. Microbiol. Biotechnol. 99 (1), 477–487.
Costa, E., et al., 2006. Why is metabolic labour divided in nitrification? Trends Microbiol. 14 (5), 213–219.
Dai, Y., et al., 2013. Effects of nitrogen application rate and a nitrification inhibitor dicyandiamide on ammonia oxidizers and N2O emissions in a grazed pasture soil. Sci. Total Environ. 465, 125–135.
Daims, H., et al., 2015. Complete nitrification by Nitrospira bacteria. Nature. 528 (7583), 504.
Daims, H., et al., 2016. A New Perspective on Microbes Formerly Known as Nitrite-Oxidizing Bacteria. Trends Microbiol. 24 (9), 699–712.
Di, H.J., Cameron, K.C., 2011. Inhibition of ammonium oxidation by a liquid formulation of 3,4-Dimethylpyrazole phosphate (DMPP) compared with a dicyandiamide (DCD) solution in six new Zealand grazed grassland soils. J. Soils Sediments. 11 (6), 1032–1039.
Di, H.J., Cameron, K.C., 2018. Ammonia oxidisers and their inhibition to reduce nitrogen losses in grazed grassland: a review. J ROY SOC NEW ZEAL. 48 (2–3), 127–142.
Di, H.J., et al., 2014. Effect of soil moisture status and a nitrification inhibitor, dicyandiamide, on ammonia oxidizer and denitrifier growth and nitrous oxide emissions in a grassland soil. Soil Biol. Biochem. 73, 59–68.
Di, H.J., et al., 2009. Nitrification driven by bacteria and not archaea in nitrogen-rich grassland soils. Nat. Geosci. 2 (9), 621–624.
Dinnes, D.L., et al., 2002. Nitrogen management strategies to reduce nitrate leaching in tile-drained midwestern soils. Agron. J. 94 (1), 153–171.
Dong, D., et al., 2018. Effects of urease and nitrification inhibitors on nitrous oxide emissions and nitrifying/denitrifying microbial communities in a rainfed maize soil: A 6-year field observation. Soil Tillage Res. 180, 82–90.
Dong, X.X., et al., 2013a. Effects of the nitrification inhibitor DMPP on soil bacterial community in a Cambisol in northeast China. J. Soil Sci. Plant Nutr. 13 (3), 580–591.
Dong, X.X., et al., 2013b. The response of nitrifier, N-fixer and denitrifier gene copy numbers to the nitrification inhibitor 3,4-dimethylpyrazole phosphate. Plant Soil Environ. 59 (9), 398–403.
Duan, Y.F., et al., 2017. Microbial N Transformations and N2O Emission after Simulated Grassland Cultivation: Effects of the Nitrification Inhibitor 3,4-Dimethylpyrazole Phosphate (DMPP). Appl. Environ. Microbiol. 83 (1), e02019–e2116.
Fan, X.P., et al., 2019. The efficacy of 3,4-dimethylpyrazole phosphate on N2O emissions is linked to niche differentiation of ammonia oxidizing archaea and bacteria across four arable soils. Soil Biol. Biochem. 130, 82–93.
Florio, A., et al., 2014. Effects of the nitrification inhibitor 3,4-dimethylpyrazole phosphate (DMPP) on abundance and activity of ammonia oxidizers in soil. Biol. Fertil. Soils. 50 (5), 795–807.
Florio, A., et al., 2016. Changes in the activity and abundance of the soil microbial community in response to the nitrification inhibitor 3,4-dimethylpyrazole phosphate (DMPP). J. Soils Sediments. 16 (12), 2687–2697.
Fowler, S.J., et al., 2018. Comammox Nitrospira are abundant ammonia oxidizers in diverse groundwater-fed rapid sand filter communities. Environ. Microbiol. 20 (3), 1002–1015.
Francis, C.A., et al., 2005. Ubiquity and diversity of ammonia-oxidizing archaea in water columns and sediments of the ocean. Proc. Natl. Acad. Sci. U. S. A. 102 (41), 14683–14688.
Fu, Q.L., et al., 2018. The short-term effects of nitrification inhibitors on the abundance and expression of ammonia and nitrite oxidizers in a long-term field experiment comparing land management. Biol. Fertil. Soils. 54 (1), 163–172.
Gilsanz, C., et al., 2016. Development of emission factors and efficiency of two nitrification inhibitors, DCD and DMPP. Agric Ecosyst Environ Agric Ecosyst Environ. 216, 1–8.
Gong, P., et al., 2013. Responses of Ammonia-Oxidizing Bacteria and Archaea in Two Agricultural Soils to Nitrification Inhibitors DCD and DMPP: A Pot Experiment. Pedosphere. 23 (6), 729–739.
Gu, Y., et al., 2019. Nitrapyrin affects the abundance of ammonia oxidizers rather than community structure in a yellow clay paddy soil. J. Soils Sediments. 19 (2), 872–882.
Guardia, G., et al., 2018. Determining the influence of environmental and edaphic factors on the fate of the nitrification inhibitors DCD and DMPP in soil. Sci. Total Environ. 624, 1202–1212.
He, J.Z., et al., 2012. Current insights into the autotrophic thaumarchaeal ammonia oxidation in acidic soils. Soil Biol. Biochem. 55, 146–154.
Hendrickson, L.L., Keeney, D.R., 1979. A bioassay to determine the effect of organic matter and pH on the effectiveness of nitrapyrin (N-Serve) as a nitrification inhibitor. Soil Biol. Biochem. 11 (1), 51–55.
Hink, L., et al., 2018. The consequences of niche and physiological differentiation of archaeal and bacterial ammonia oxidisers for nitrous oxide emissions. ISME J. 12 (4), 1084–1093.
Hirzel, J., et al., 2012. Soil potentially mineralizable nitrogen and its relation to rice production and nitrogen needs in two paddy rice soils of chile. J Plant Nutr. 35 (3), 396–412.
Ho, R., 2006. Handbook of univariate and multivariate data analysis and interpretation with SPSS. CRC Press.
Hu, H.W., et al., 2015a. Microbial regulation of terrestrial nitrous oxide formation: understanding the biological pathways for prediction of emission rates. FEMS Microbiol. Rev. 39 (5), 729–749.
Hu, H.W., et al., 2015b. The large-scale distribution of ammonia oxidizers in paddy soils is driven by soil pH, geographic distance, and climatic factors. Front. Microbiol. 6, 938.
Huang, X., et al., 2018. Neutrophilic bacteria are responsible for autotrophic ammonia oxidation in an acidic forest soil. Soil Biol. Biochem. 119, 83–89.
Huang, Y., et al., 2014. Nitrate enhances N2O emission more than ammonium in a highly acidic soil. J. Soils Sediments. 14 (1), 146–154.
Jia, Z.J., Conrad, R., 2009. Bacteria rather than Archaea dominate microbial ammonia oxidation in an agricultural soil. Environ. Microbiol. 11 (7), 1658–1671.
Jiang, X., et al., 2015. pH regulates key players of nitrification in paddy soils. Soil Biol. Biochem. 81, 9–16.
Kits, K.D., et al., 2017. Kinetic analysis of a complete nitrifier reveals an oligotrophic lifestyle. Nature. 549 (7671), 269-+.
Kleineidam, K., et al., 2011. Influence of the nitrification inhibitor 3,4-dimethylpyrazole phosphate (DMPP) on ammonia-oxidizing bacteria and archaea in rhizosphere and bulk soil. Chemosphere. 84 (1), 182–186.
Kool, D.M., et al., 2011. Nitrifier denitrification as a distinct and significant source of nitrous oxide from soil. Soil Biol. Biochem. 43 (1), 174–178.
Kool, D.M., et al., 2010. Nitrifier denitrification can be a source of N2O from soil: a revised approach to the dual-isotope labelling method. Eur J Soil Sci. 61 (5), 759–772.
Kou, Y.P., et al., 2015. Effects of 3, 4-dimethylpyrazole phosphate and dicyandiamide on nitrous oxide emission in a greenhouse vegetable soil. Plant Soil Environ. 61 (1), 29–35.

Kozlowski, J.A., et al., 2016. Pathways and key intermediates required for obligate aerobic ammonia-dependent chemolithotrophy in bacteria and Thaumarchaeota. ISME J. 10 (8), 1836–1845.
Kumar, S., et al., 2004. MEGA3: Integrated software for molecular evolutionary genetics analysis and sequence alignment. Brief. Bioinform. 5 (2), 150–163.
Lan, T., et al., 2018. Effects of nitrification inhibitors on gross N nitrification rate, ammonia oxidizers, and N2O production under different temperatures in two pasture soils. Environ. Sci. Pollut. Res. 25 (28), 28344–28354.
Lawton, T.J., et al., 2014. Structural conservation of the B subunit in the ammonia monooxygenase/particulate methane monooxygenase superfamily. Proteins. 82 (9), 2263–2267.
Li, C.Y., et al., 2019a. Comammox Nitrospira play an active role in nitrification of agricultural soils amended with nitrogen fertilizers. Soil Biol. Biochem. 138, 107609.
Li, J., et al., 2019b. Effects of 3,4-dimethylpyrazole phosphate (DMPP) on the abundance of ammonia oxidizers and denitrifiers in two different intensive vegetable cultivation soils. J. Soils Sediments. 19 (3), 1250–1259.
Li, Y.W., et al., 2020. Salinity-induced concomitant increases in soil ammonia volatilization and nitrous oxide emission. Geoderma. 361 (10), 114053.
Marsden, K.A., et al., 2016. The mobility of nitrification inhibitors under simulated ruminant urine deposition and rainfall: a comparison between DCD and DMPP. Biol. Fertil. Soils. 52 (4), 491–503.
McCarty, G.W., 1999. Modes of action of nitrification inhibitors. Biol. Fertil. Soils. 29 (1), 1–9.
Medinets, S., et al., 2015. A review of soil NO transformation: Associated processes and possible physiological significance on organisms. Soil Biol. Biochem. 80, 92–117.
Meinhardt, K.A., et al., 2018. Ammonia-oxidizing bacteria are the primary N2O producers in an ammonia-oxidizing archaea dominated alkaline agricultural soil. Environ. Microbiol. 20 (6), 2195–2206.
Menéndez, S., et al., 2012. Efficiency of nitrification inhibitor DMPP to reduce nitrous oxide emissions under different temperature and moisture conditions. Soil Biol. Biochem. 53, 82–89.
Misselbrook, T.H., et al., 2014. An assessment of nitrification inhibitors to reduce nitrous oxide emissions from UK agriculture. Environ. Res. Lett. 9 (11), 115006.
Morales, S.E., et al., 2015. Impact of urine and the application of the nitrification inhibitor DCD on microbial communities in dairy-grazed pasture soils. Soil Biol. Biochem. 88, 344–353.
Müller, C., et al., 2002. The nitrification inhibitor DMPP had no effect on denitrifying enzyme activity. Soil Biol. Biochem. 34 (11), 1825–1827.
Palomo, A., et al., 2016. Metagenomic analysis of rapid gravity sand filter microbial communities suggests novel physiology of Nitrospira spp. ISME J. 10 (11), 2569–2581.
Palomo, A., et al., 2018. Comparative genomics sheds light on niche differentiation and the evolutionary history of comammox Nitrospira. ISME J. 12 (7), 1779–1793.
Pinto, A.J., et al., 2016. Metagenomic Evidence for the Presence of Comammox Nitrospira-Like Bacteria in a Drinking Water System. Msphere. 1 (1), e00054–e115.
Pjevac, P., et al., 2017. AmoA-Targeted Polymerase Chain Reaction Primers for the Specific Detection and Quantification of Comammox Nitrospirain the Environment. Front. Microbiol. 8, 1508.
Prosser, J.I., Nicol, G.W., 2012. Archaeal and bacterial ammonia-oxidisers in soil: the quest for niche specialisation and differentiation. Trends Microbiol. 20 (11), 523–531.
Qiao, C.L., et al., 2015. How inhibiting nitrification affects nitrogen cycle and reduces environmental impacts of anthropogenic nitrogen input. Glob Chang Biol. 21 (3), 1249–1257.
Ravishankara, A.R., et al., 2009. Nitrous Oxide (N2O): The Dominant Ozone-Depleting Substance Emitted in the 21st Century. Science. 326 (5949), 123–125.
Rotthauwe, J.H., et al., 1997. The ammonia monooxygenase structural gene amoA as a functional marker: Molecular fine-scale analysis of natural ammonia-oxidizing populations. Appl. Environ. Microbiol. 63 (12), 4704–4712.
Ruser, R., Schulz, R., 2015. The effect of nitrification inhibitors on the nitrous oxide (N2O) release from agricultural soils-a review. J. Plant. Nutr. Soil Sci. 178 (2), 171–188.
Sahrawat, K.L., 2008. Factors affecting nitrification in soils. Commun Soil Sci Plant Anal. 39 (9–10), 1436–1446.
Schlesinger, W.H., 2009. On the fate of anthropogenic nitrogen. Proc. Natl. Acad. Sci. U.S.A. 106 (1), 203–208.
Shaw, L.J., et al., 2006. Nitrosospira spp. can produce nitrous oxide via a nitrifier denitrification pathway. Environ. Microbiol. 8 (2), 214–222.
Shen, J.P., et al., 2008. Abundance and composition of ammonia-oxidizing bacteria and ammonia-oxidizing archaea communities of an alkaline sandy loam. Environ. Microbiol. 10 (6), 1601–1611.
Shen, T.L., et al., 2013. Responses of the terrestrial ammonia-oxidizing archaeon Ca. Nitrososphaera viennensis and the ammonia-oxidizing bacterium Nitrosospira multiformis to nitrification inhibitors. FEMS Microbiol. Lett. 344 (2), 121–129.
Shi, X.Z., et al., 2016a. Effects of 3,4-dimethylpyrazole phosphate (DMPP) on nitrification and the abundance and community composition of soil ammonia oxidizers in three land uses. Biol. Fertil. Soils. 52 (7), 927–939.
Shi, X.Z., et al., 2016b. Effects of the Nitrification Inhibitor 3,4-Dimethylpyrazole Phosphate on Nitrification and Nitrifiers in Two Contrasting Agricultural Soils. Appl. Environ. Microbiol. 82 (17), 5236–5248.
Shi, X.Z., et al., 2017. Nitrifier-induced denitrification is an important source of soil nitrous oxide and can be inhibited by a nitrification inhibitor 3,4-dimethylpyrazole phosphate. Environ. Microbiol. 19 (12), 4851–4865.
Soares, J.R., et al., 2016. Nitrous oxide emission related to ammonia-oxidizing bacteria and mitigation options from N fertilization in a tropical soil. Sci. Rep. 6, 30349.
Subbarao, G.V., et al., 2009. Evidence for biological nitrification inhibition in Brachiaria pastures. Proc. Natl. Acad. Sci. U.S.A. 106 (41), 17302–17307.
Subbarao, G.V., et al., 2008. Free fatty acids from the pasture grass Brachiaria humidicola and one of their methyl esters as inhibitors of nitrification. Plant Soil. 313 (1–2), 89–99.
Thapa, R., et al., 2016. Effect of Enhanced Efficiency Fertilizers on Nitrous Oxide Emissions and Crop Yields: A Meta-analysis. Soil Sci Soc Am J. 80 (5), 1121–1134.
Tolar, B.B., et al., 2017. Integrated structural biology and molecular ecology of N-cycling enzymes from ammonia-oxidizing archaea. Environ. Microbiol. Rep. 9 (5), 484–491.
Tourna, M., et al., 2011. Nitrososphaera viennensis, an ammonia oxidizing archaeon from soil. Proc. Natl. Acad. Sci. U.S.A. 108 (20), 8420–8425.
Ussiri, D., Lal, R., 2012. Soil emission of nitrous oxide and its mitigation. Springer Science & Business Media.
van Kessel, M., et al., 2015. Complete nitrification by a single microorganism. Nature. 528 (7583), 555-+.
Verhamme, D.T., et al., 2011. Ammonia concentration determines differential growth of ammonia-oxidising archaea and bacteria in soil microcosms. ISME J. 5 (6), 1067–1071.
Wang, Q., et al., 2017a. Effects of the nitrification inhibitor dicyandiamide (DCD) on N2O emissions and the abundance of nitrifiers and denitrifiers in two contrasting agricultural soils. J. Soils Sediments. 17 (6), 1635–1643.
Wang, Q., et al., 2016a. Effects of dicyandiamide and acetylene on N2O emissions and ammonia oxidizers in a fluvo-aquic soil applied with urea. Environ. Sci. Pollut. Res. 23 (22), 23023–23033.
Wang, Q., et al., 2016b. Nitrogen fertiliser-induced changes in N2O emissions are attributed more to ammonia-oxidising bacteria rather than archaea as revealed using 1-octyne and acetylene inhibitors in two arable soils. Biol. Fertil. Soils. 52 (8), 1163–1171.
Wang, Y., et al., 2017b. Comammox in drinking water systems. Water Res. 116, 332–341.
Wang, Z.H., et al., 2019. Comammox Nitrospira clade B contributes to nitrification in soil. Soil Biol. Biochem. 135, 392–395.
Woodward, E.E., et al., 2016. Nitrapyrin in Streams: The First Study Documenting Off-Field Transport of a Nitrogen Stabilizer Compound. Environ. Sci. Technol. Lett. 3 (11), 387–392.
Wu, D., et al., 2017. Nitrification inhibitors mitigate N2O emissions more effectively under straw-induced conditions favoring denitrification. Soil Biol. Biochem. 104, 197–207.
Wu, D., et al., 2018. Potential dual effect of nitrification inhibitor 3,4-dimethylpyrazole phosphate on nitrifier denitrification in the mitigation of peak N2O emission events in North China Plain cropping systems. Soil Biol. Biochem. 121, 147–153.
Wu, Y., et al., 2011. Long-term field fertilization significantly alters community structure of ammonia-oxidizing bacteria rather than archaea in a paddy soil. Soil Sci Soc Am J. 75 (4), 1431–1439.
Xia, F., et al., 2018. Ubiquity and Diversity of Complete Ammonia Oxidizers (Comammox). Appl. Environ. Microbiol. 84 (24), e01390–e1418.
Xia, W.W., et al., 2011. Autotrophic growth of nitrifying community in an agricultural soil. ISME J. 5 (7), 1226–1236.
Xu, J., et al., 2012. Ammonia volatilization losses from a rice paddy with different irrigation and nitrogen managements. Agric Water Manag. 104, 184–192.
Zerulla, W., et al., 2001. 3,4-Dimethylpyrazole phosphate (DMPP) – a new nitrification inhibitor for agriculture and horticulture. Biol. Fertil. Soils. 34 (2), 79–84.
Zhang, H.J., et al., 2004. Dicyandiamide sorption-desorption behavior on soils and peat humus. Pedosphere. 14 (3), 395–399.
Zhang, L.M., et al., 2012. Ammonia-oxidizing archaea have more important role than ammonia-oxidizing bacteria in ammonia oxidation of strongly acidic soils. ISME J. 6 (5), 1032–1045.
Zhang, M.Y., et al., 2018. Antagonistic effects of nitrification inhibitor 3,4-dimethylpyrazole phosphate and fungicide iprodione on net nitrification in an agricultural soil. Soil Biol. Biochem. 116, 167–170.
ŠImek, M., Cooper, J.E., 2002. The influence of soil pH on denitrification: progress towards the understanding of this interaction over the last 50 years. Eur. J. Soil Sci. 53 (3), 345–354.

**Supplementary material**

**Table S1** Quantitative PCR protocols.

| Target gene | Primer (5'-3') | Quantitative PCR protocol | Reference |
|---|---|---|---|
| AOA *amoA* | Arch-amoAF<br>STAATGGTCTGGCTTAGACG | 95°C, 3min; 40×(95°C, 30s; 55°C ,30s; 74°C, 30s with plate read); Melt curve 65.0°C to 95.0°C, increment 0.5°C, 0:05+ plate read | (Tourna et al., 2008) |
| | Arch-amoAR<br>GCGGCCATCCATCTGTATGT | | |
| AOB *amoA* | amoA1F<br>GGGGTTTCTACTGGTGGT | 95°C, 3min; 40×(95°C, 30s; 55°C ,30s; 74°C, 30s with plate read); Melt curve 65.0°C to 95.0°C, increment 0.5°C, 0:05+ plate read | (Rotthauwe et al., 1997) |
| | amoA2R<br>CCCCTCKGSAAAGCCTTCTTC | | |
| Comammox Nitrospira clade A *amoA* | comaA-244f_a<br>TACAACTGGGTGAACTA<br>comaA-244f_b<br>TATAACTGGGTGAACTA<br>comaA-244f_c<br>TACAATTGGGTGAACTA<br>comaA-244f_d<br>TACAACTGGGTCAACTA<br>comaA-244f_e<br>TACAACTGGGTCAATTA<br>comaA-244f_f<br>TATAACTGGGTCAATTA | 95°C, 3min; 45×(95°C, 30s; 52°C, 45s; 72°C, 1min with plate read); Melt curve 38.0°C to 96.0°C, increment 0.5°C, 0:05+ plate read | (Pjevac et al., 2017) |
| | comaA-659r_a<br>AGATCATGGTGCTATG<br>comaA-659r_b<br>AAATCATGGTGCTATG<br>comaA-659r_c<br>AGATCATGGTGCTGTG<br>comaA-659r_d<br>AAATCATGGTGCTGTG<br>comaA-659r_e<br>AGATCATCGTGCTGTG<br>comaA-659r_f<br>AAATCATCGTGCTGTG | | |

**Table S2** Accession numbers of comammox clone in Fig. S2.

| Clone | Accession number |
|---|---|
| 1 | MK537313 |
| 2 | MK537315 |
| 3 | MK537305 |
| 4 | MK537312 |
| 5 | MK537314 |
| 6 | MK537306 |
| 7 | MK537308 |
| 8 | MK537307 |
| 9 | MK537311 |
| 10 | MK537309 |
| 11 | MK537310 |

**Table S3** Significant effects of incubation date, soil type and fertilizer type (control, urea, DCD, DMPP and nitrapyrin) on $N_2O$, $NH_4^+$, $NO_3^-$, AOA and AOB (three-way ANOVA day×soil×fertilizer). '*' represents the significant difference ($P < 0.05$).

| Main Factor | $N_2O$ | | $NH_4^+$ | | $NO_3^-$ | | AOA | | AOB | |
|---|---|---|---|---|---|---|---|---|---|---|
| | F | P | F | P | F | P | F | P | F | P |
| day | 493.637 | * | 105.475 | * | 1974 | * | 294.88 | * | 452.232 | * |
| soil | 89.341 | * | 2813 | * | 3524 | * | 635.85 | * | 59.551 | * |
| fertilizer | 1182 | * | 431.891 | * | 661.313 | * | 120.829 | * | 834.187 | * |
| day×soil | 117.881 | * | 8.912 | * | 62.938 | * | 254.252 | * | 15.835 | * |
| day×fertilizer | 294.941 | * | 7.164 | * | 134.225 | * | 33.484 | * | 467.35 | * |
| soil×fertilizer | 117.151 | * | 62.701 | * | 254.11 | * | 68.274 | * | 21.862 | * |
| day×soil×fertilizer | 131.064 | * | 4.732 | * | 59.833 | * | 31.529 | * | 9.289 | * |

**Table S4** P-value and pearson correlation coefficient of multivariate analyses between nitrifier abundance and N dynamics ($N_2O$, $NH_4^+$ and $NO_3^-$ concentration).

| Soil | Treatment | Nitrifier abundance | N2O | | NH4 | | NO3 | |
|---|---|---|---|---|---|---|---|---|
| | | | r | *P* | r | *P* | r | *P* |
| HL | control | AOA | -0.82 | 0.38 | -0.23 | 0.85 | 1.00 | 0.01 |
| | | AOB | 0.83 | 0.38 | 0.22 | 0.86 | -1.00 | 0.02 |
| | | comammox | -0.16 | 0.90 | 0.98 | 0.14 | -0.45 | 0.71 |
| | urea | AOA | 0.41 | 0.73 | 0.40 | 0.74 | 0.70 | 0.51 |
| | | AOB | 0.99 | 0.07 | -0.59 | 0.60 | 0.97 | 0.16 |
| | | comammox | -0.70 | 0.51 | -0.06 | 0.96 | -0.90 | 0.29 |
| | DCD | AOA | -0.87 | 0.33 | -0.79 | 0.42 | 0.76 | 0.45 |
| | | AOB | -0.97 | 0.15 | -0.17 | 0.89 | 0.11 | 0.93 |
| | | comammox | -0.90 | 0.29 | -0.75 | 0.46 | 0.71 | 0.49 |
| | DMPP | AOA | -0.86 | 0.34 | -0.65 | 0.55 | 0.76 | 0.45 |
| | | AOB | 0.27 | 0.82 | 1.00 | 0.06 | -1.00 | 0.04 |
| | | comammox | 0.05 | 0.97 | 0.99 | 0.09 | -0.96 | 0.18 |
| | Nitrapyrin | AOA | -0.83 | 0.37 | -0.90 | 0.28 | 0.87 | 0.32 |
| | | AOB | 0.79 | 0.42 | 0.93 | 0.23 | -0.91 | 0.28 |
| | | comammox | -0.90 | 0.28 | -0.83 | 0.38 | 0.79 | 0.42 |
| JX | control | AOA | -0.94 | 0.23 | 0.28 | 0.82 | 0.36 | 0.76 |
| | | AOB | 0.78 | 0.43 | 0.05 | 0.97 | -0.64 | 0.55 |
| | urea | AOA | -0.77 | 0.45 | -0.96 | 0.18 | 0.99 | 0.09 |
| | | AOB | 0.70 | 0.51 | -0.21 | 0.86 | 0.08 | 0.95 |
| | DCD | AOA | -0.57 | 0.61 | -0.91 | 0.27 | 0.86 | 0.34 |
| | | AOB | 0.45 | 0.70 | 0.84 | 0.36 | -0.78 | 0.43 |
| | DMPP | AOA | -0.90 | 0.29 | -0.96 | 0.17 | 0.93 | 0.24 |
| | | AOB | 0.49 | 0.68 | 0.95 | 0.21 | -0.97 | 0.15 |
| | Nitrapyrin | AOA | -0.95 | 0.21 | -0.76 | 0.45 | 1.00 | 0.06 |
| | | AOB | -0.40 | 0.74 | -0.99 | 0.09 | 0.74 | 0.47 |
| SC | control | AOA | 0.89 | 0.30 | 0.90 | 0.29 | -0.98 | 0.13 |
| | | AOB | -0.95 | 0.20 | -0.95 | 0.21 | 0.84 | 0.37 |
| | urea | AOA | -0.73 | 0.48 | -0.78 | 0.43 | 0.92 | 0.26 |
| | | AOB | 0.84 | 0.36 | 0.65 | 0.55 | -0.83 | 0.37 |
| | DCD | AOA | -0.30 | 0.81 | -0.93 | 0.25 | 0.99 | 0.10 |
| | | AOB | 0.03 | 0.98 | 0.99 | 0.07 | -0.90 | 0.28 |
| | DMPP | AOA | -0.19 | 0.88 | -0.96 | 0.18 | 0.96 | 0.19 |
| | | AOB | 0.20 | 0.87 | 0.96 | 0.17 | -0.96 | 0.18 |
| | Nitrapyrin | AOA | -0.98 | 0.13 | -1.00 | 0.06 | 1.00 | 0.04 |
| | | AOB | 0.96 | 0.18 | 0.92 | 0.25 | -0.91 | 0.27 |

**Figure S1** Agarose gel electrophoresis of Comammox clade A *amoA* gene in HL soil under microcosm incubation.

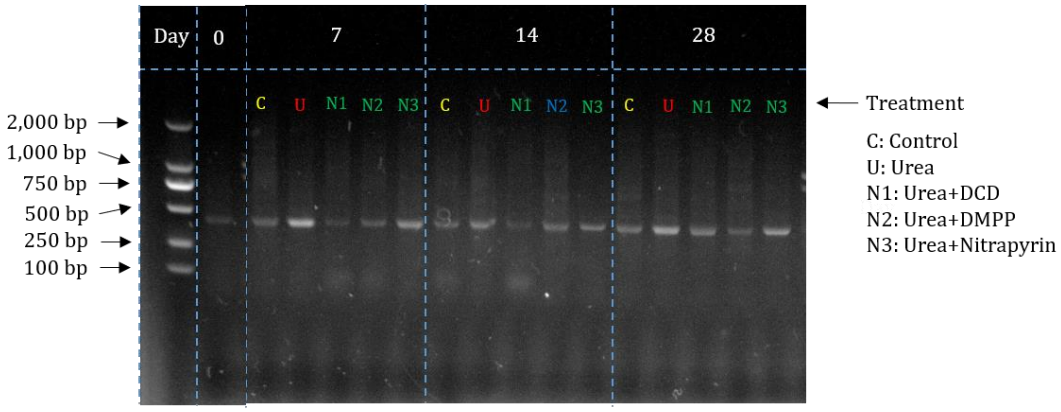

**Figure S2** Phylogenetic analysis of the comammox *amoA* gene retrieved from the DNA-SIP heavy fractions in the HL soil. Neighbor-joining analysis was performed with 1,000 bootstrap replicates to infer tree topology. Bootstrap values higher than 60% are indicated at branch nodes. The scale bar represents nucleotide acid substitution percentage.

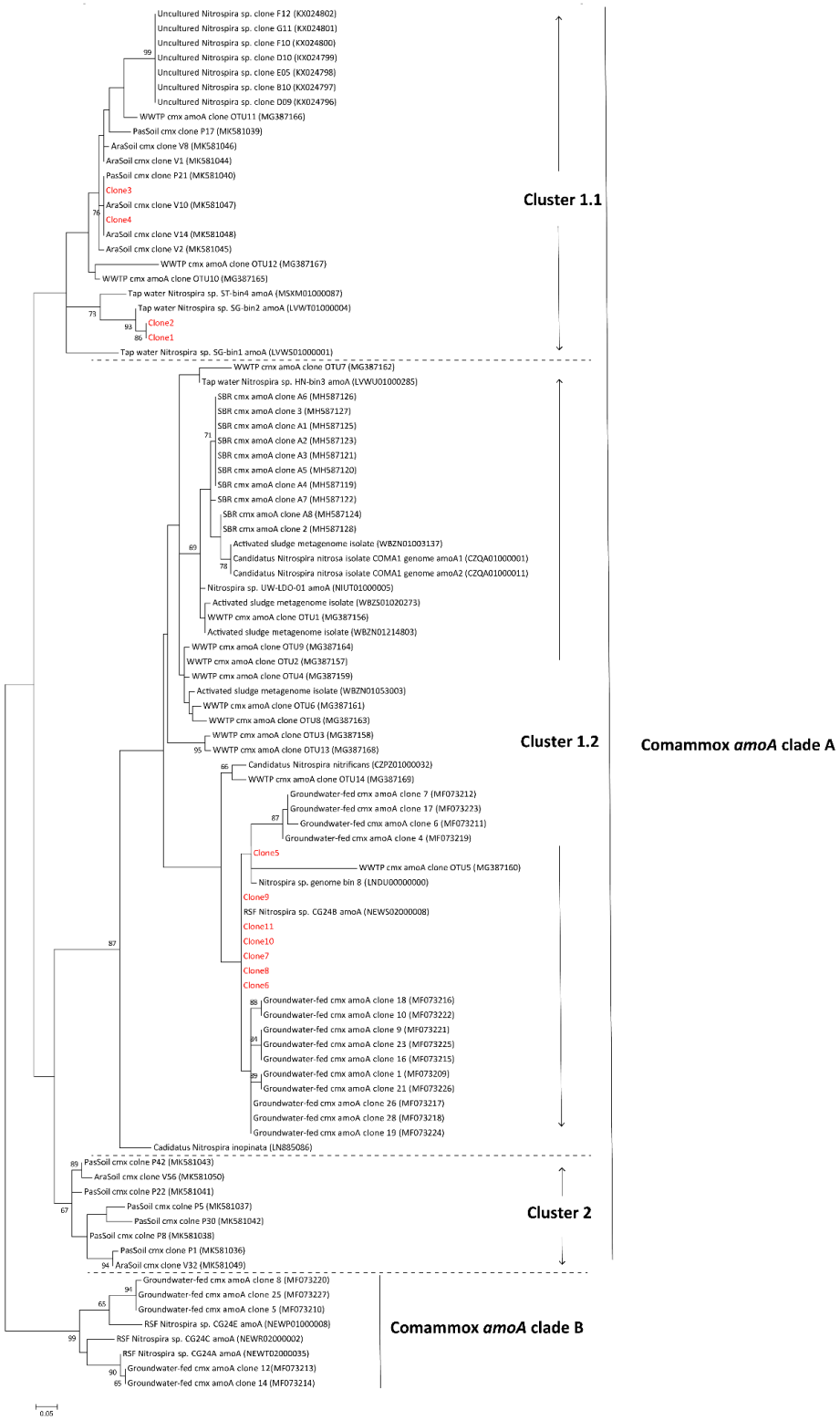

**Figure S3** Pearson correlation analysis between N dynamics ($N_2O$, $NH_4^+$ and $NO_3^-$ concentration) and AOA abundance in HL. The arrows indicated the time evolution.

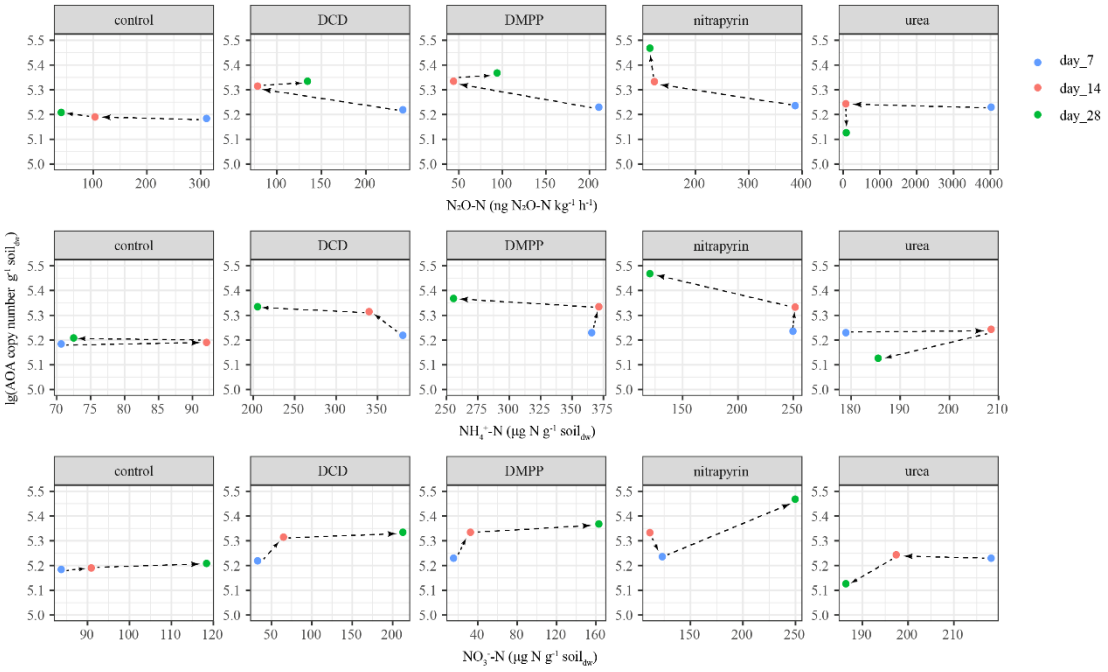

**Figure S4** Pearson correlation analysis between N dynamics ($N_2O$, $NH_4^+$ and $NO_3^-$ concentration) and AOB abundance in HL. The arrows indicated the time evolution.

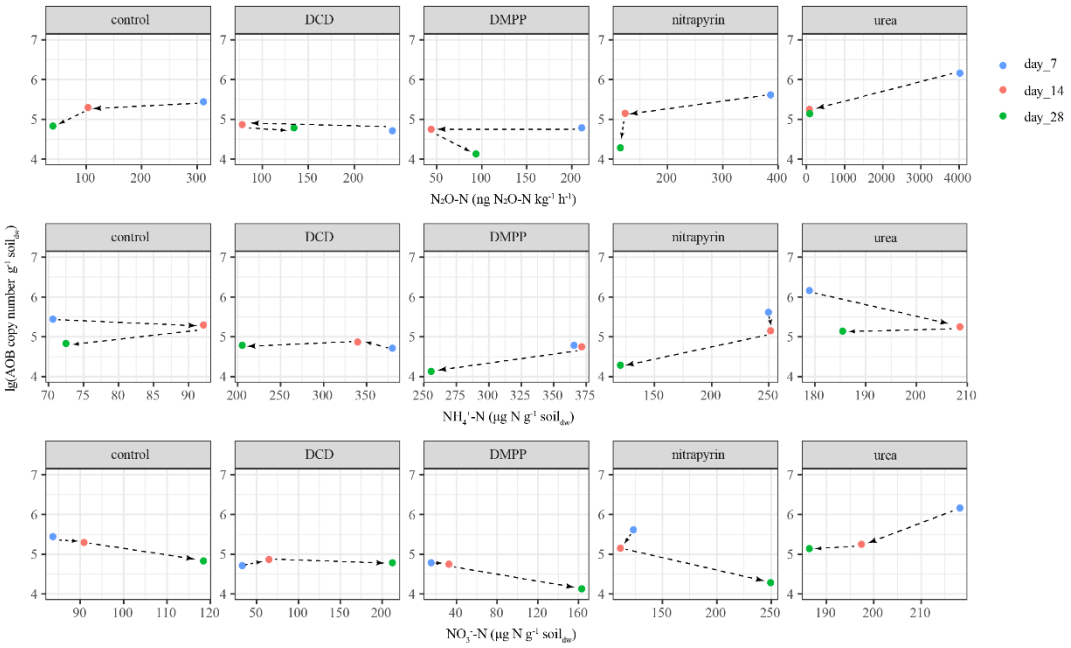

**Figure S5** Pearson correlation analysis between N dynamics ($N_2O$, $NH_4^+$ and $NO_3^-$ concentration) and comammox abundance in HL. The arrows indicated the time evolution.

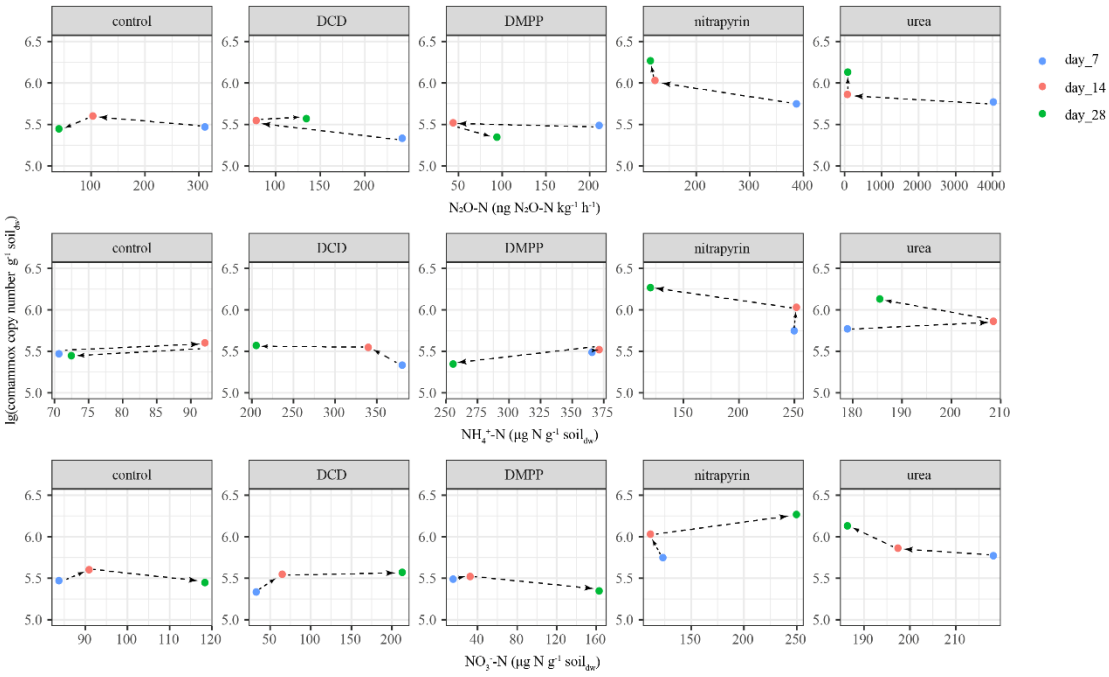

**Figure S6** Pearson correlation analysis between N dynamics ($N_2O$, $NH_4^+$ and $NO_3^-$ concentration) and AOA abundance in JX. The arrows indicated the time evolution.

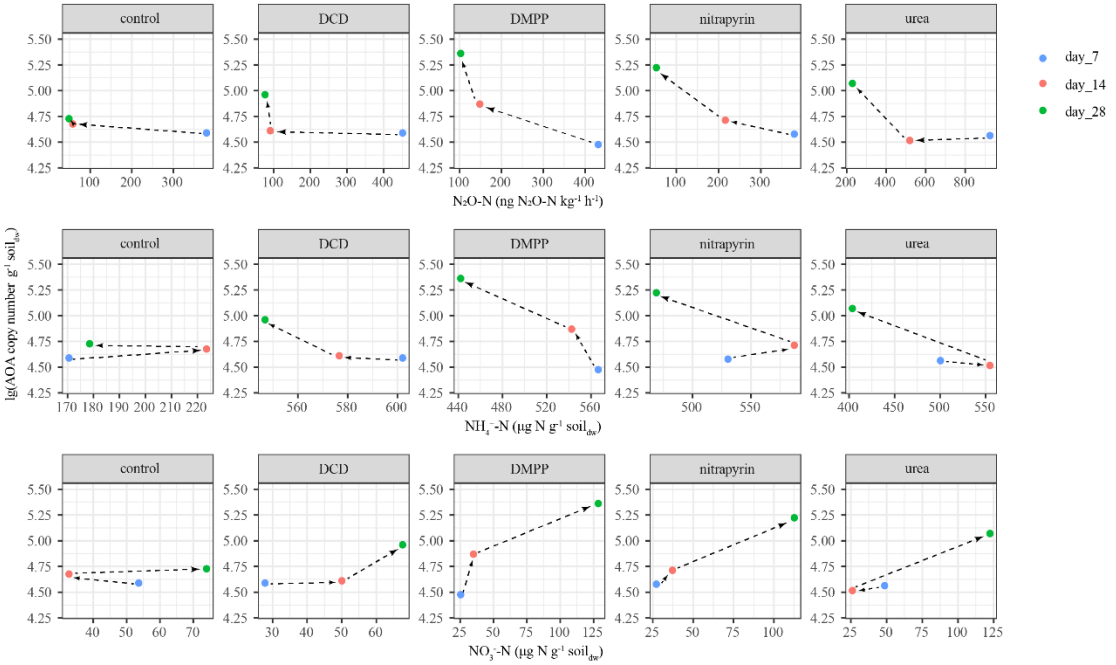

**Figure S7** Pearson correlation analysis between N dynamics ($N_2O$, $NH_4^+$ and $NO_3^-$ concentration) and AOB abundance in JX. The arrows indicated the time evolution.

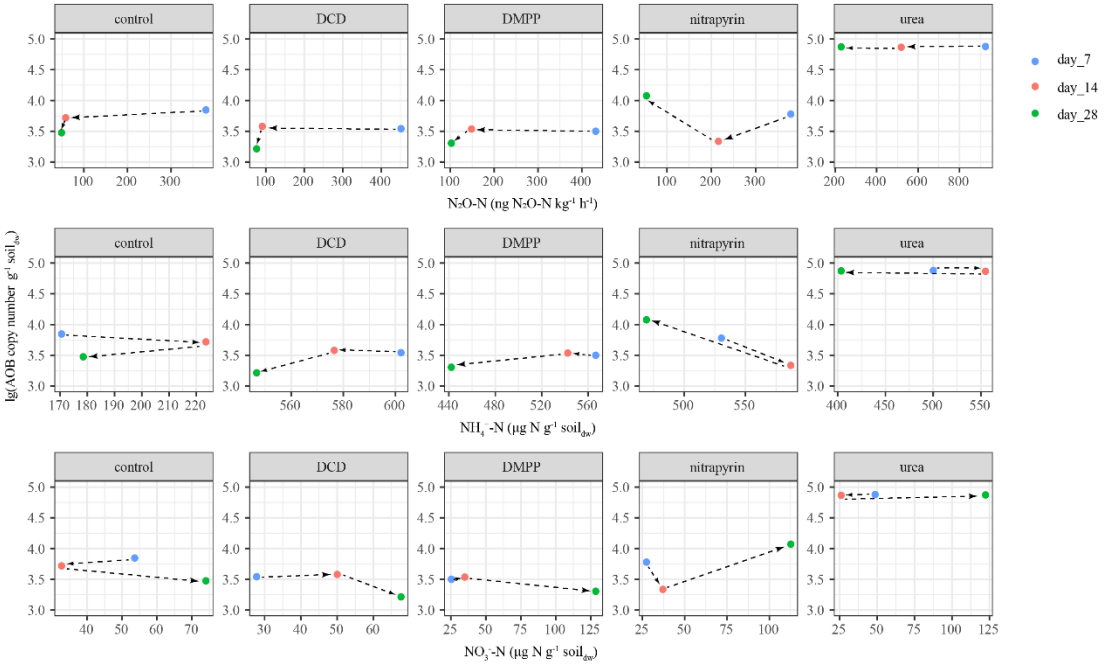

**Figure S8** Pearson correlation analysis between N dynamics ($N_2O$, $NH_4^+$ and $NO_3^-$ concentration) and AOA abundance in SC. The arrows indicated the time evolution.

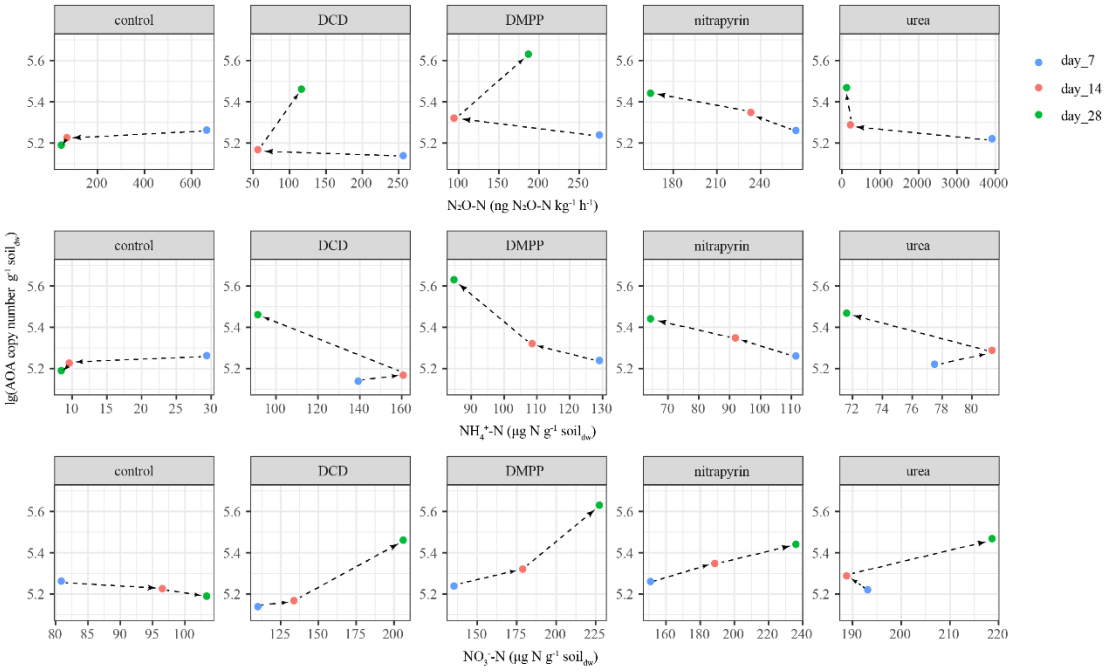

**Figure S9** Pearson correlation analysis between N dynamics ($N_2O$, $NH_4^+$ and $NO_3^-$ concentration) and AOB abundance in SC. The arrows indicated the time evolution.

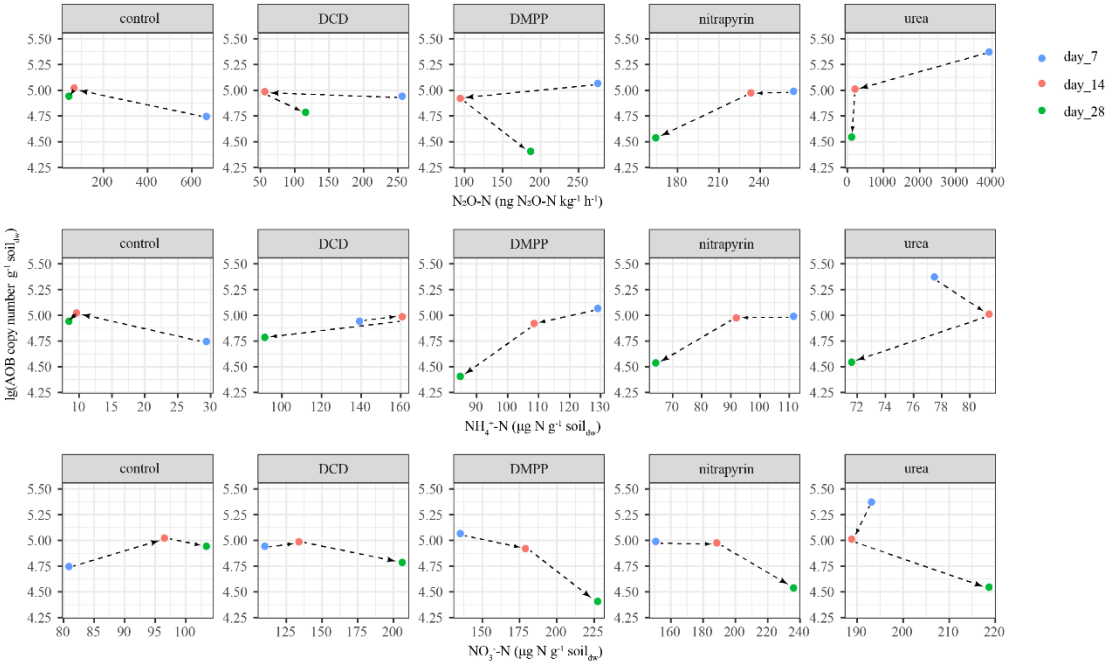

**Figure S10** Changes in $N_2O$ during SIP-incubation of soil microcosms for 7, 14, 21 and 28 days in HL (A) and JX (B) soil. Microcosms were amended with urea, and urea with NIs (DCD, DMPP and nitrapyrin, respectively). $N_2O$ was analyzed before opening and $N_2O$ production rates were calculated as described in the Materials and Methods section. Mean concentration and standard errors of triplicate microcosms are presented. The different lowercase letter indicated the significant difference between different fertilizer treatments at each time point within the same soil; the different capital letters indicated the significant difference between each time point in the same fertilizer treatment within the same soil.

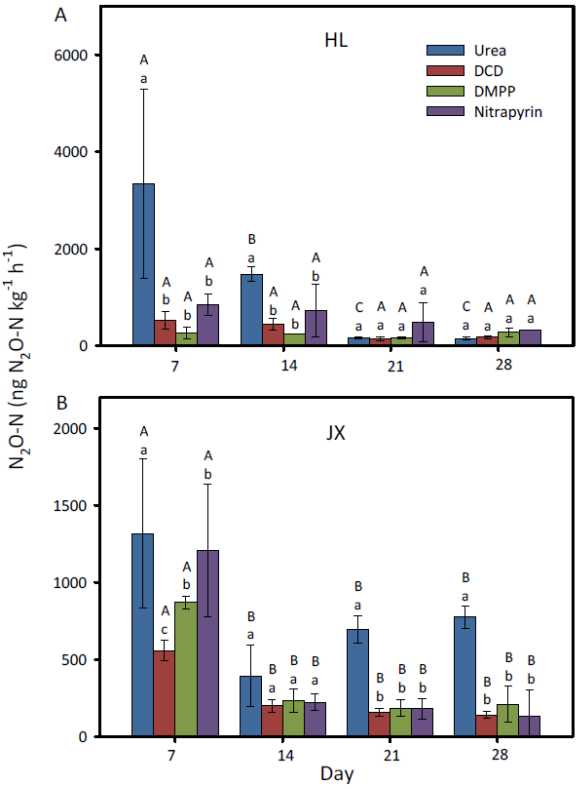

**Figure S11** Changes in the abundance of archaeal (A, D), bacterial (B, E) and comammox (C) *amoA* genes during incubation of HL (A, B, C) and JX (D, E) soil microcosms. Quantitation was performed from destructively sampled soil microcosms incubated for 14 and 28 days that were amended with urea, and urea with NIs (DCD, DMPP and nitrapyrin, respectively). Mean concentration and standard errors of triplicate microcosms are presented. The different lowercase letter indicated the significant difference between different fertilizer treatments at each time point within the same soil; the different capital letters indicated the significant difference between each time point in the same fertilizer treatment within the same soil.

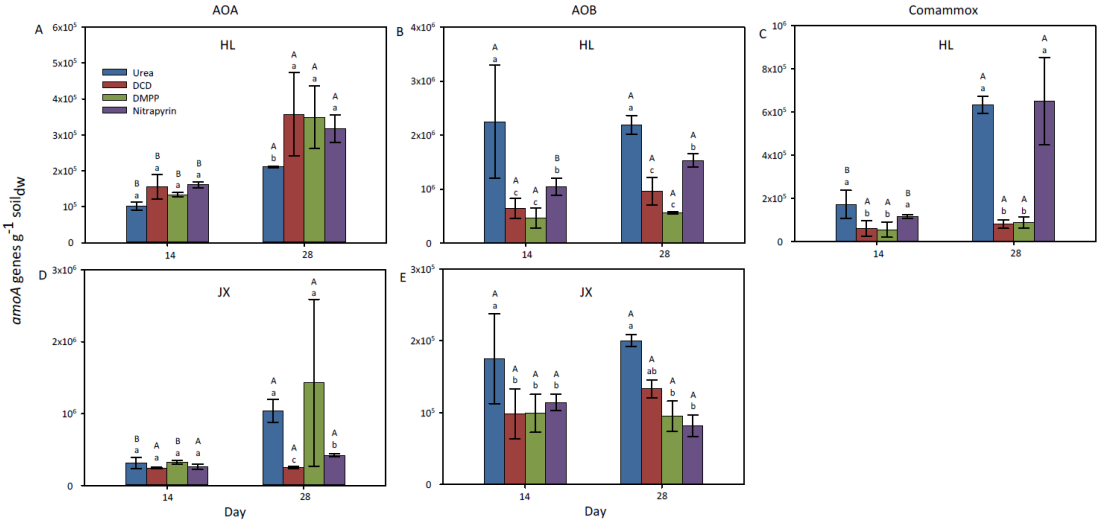


Reference:

Pjevac, P et al., 2017. AmoA-Targeted Polymerase Chain Reaction Primers for the Specific Detection and Quantification of ComammoxNitrospirain the Environment. Front. Microbiol. 8, 1508.

Rotthauwe, J.H et al., 1997. The ammonia monooxygenase structural gene amoA as a functional marker: Molecular fine-scale analysis of natural ammonia-oxidizing populations. Appl. Environ. Microbiol. 63(12), 4704-4712.

Tourna, M et al., 2008. Growth, activity and temperature responses of ammonia-oxidizing archaea and bacteria in soil microcosms. Environ. Microbiol. 10(5), 1357-1364.